Computer Model for a Towed Submarine Communication Antenna

by

Gary A. Ulrich
B.S., Moorhead State University (1986)

Submitted to the Department of Ocean Engineering and the Department of Mechanical Engineering in partial fulfillment of the requirements for the degrees of

Naval Engineer
and
Master of Science in Mechanical Engineering

at the
MASSACHUSETTS INSTITUTE OF TECHNOLOGY
June 1999

Signature of Author Gary A Ulrich
Department of Ocean Engineering
13 May, 1999

Certified by Jerome H. Milgram
Jerome H. Milgram
Professor, Ocean Engineering
Thesis Supervisor

Certified by
Ain A. Sonin
Professor, Mechanical Engineering
Thesis Reader

Accepted by Arthur B Baggeroer
Art Baggeroer
Ford Professor of Engineering
Chairman of Committee on Graduate Studies, Ocean Engineering Department

Accepted by
Ain A. Sonin
Chairman of Committee on Graduate Studies, Mechanical Engineering Department

Computer Model for a Towed Submarine Communication Antenna

by

Gary A. Ulrich

Submitted to the Department of Ocean Engineering
on 13 May 1993, in partial fulfillment of the
requirements for the degree of
Naval Engineer
Master of Science, Mechanical Engineering

Abstract

A finite difference computer model is developed to simulate the exposure statistics of a radio frequency buoyant antenna as it is towed in a random seaway. The model allows the user to prescribe antenna properties (length, diameter, density, etc.), sea conditions (significant wave height, development of sea), and tow speed. The model then simulates the antenna-sea interaction for the desired duration to collect statistics relating to antenna performance. The model provides design engineers with a tool to predict antenna performance trends, and conduct design tradeoff studies. The antenna envisioned is a submarine floating antenna which would enable communications at speed and depth, greatly enhancing the stealth and survivability of the US Navy's submarine force.

Thesis Supervisor: Jerome H. Milgram
Title: Professor, Ocean Engineering

Thesis Supervisor: Ain A. Sonin
Title: Professor, Mechanical Engineering

Contents

List of Tables

List of Figures

Chapter 1

Introduction

Driven largely by demand in the commercial sector, the capability for high speed data transfer has grown at an amazing rate over the last few years. Recently deployed military communications systems have been able to leverage off their commercial counterparts to some extent, and now operate at higher frequencies and data rates than the systems they have replaced. However, the United States submarine force faces unique challenges in fully utilizing systems which operate at higher frequencies. Submarine operations are typically driven by the need for stealth, and stealth is best preserved by remaining fully submerged. Currently submarine communications can be typified by a pattern of coming to periscope depth periodically to raise a radio mast, send or receive required message traffic, then submerge. While submerged, radio communications systems are limited to low data rate receive-only modes transmitted at very low frequencies (ELF or VLF bands). Clearly, the communications goal of the submarine force is to be able to utilize the high frequency (UHF, SHF, or EHF bands) and high data rate communication circuits while retaining the stealth of operation at depth.

This goal of high data rate communication at depth was the motivation of a U. S. Navy Advanced Technology Demonstration (ATD). Initially funded jointly by DARPA and ONR in FY 96-97 as a feasibility study, the Buoyant Cable Array Antenna research became a DARPA/ONR Demonstration in FY 98. The program was promoted to the level of Navy ATD in FY 00. This ATD, one of only 6 ATD's funded by the Navy for fiscal year 2000, reflects the high priority the Navy places on submarine connectivity. The goals of the program include [1]

- verify the capability to conduct beamforming signal processing
- verify adequate antenna performance and gain in a seaway
- develop transmit capability
- conduct design studies on key antenna characteristics (diameter, length, density, etc.)

In addition to the engineering challenges inherent in any new design work, the program manager must ensure the designers keep system affordability and flexibility in mind.

1.1 Background

Lincoln Laboratory is a federally funded laboratory administered by Massachusetts Institute of Technology. Lincoln Lab, specializing in radar and electrical engineering, is well qualified to tackle the challenge of designing a floating linear array RF communication antenna. However, to better characterize the behavior of the antenna in a random seaway, Lincoln Lab added Professor Jerome Milgram of the MIT Ocean Engineering department to the antenna development effort. Professor Milgram was made the head of the Exposure Statistics Working Group, whose charter was to develop a model to provide statistics on

- the average fraction of antenna elements exposed over an extended period of time
- the temporal variation of the exposure statistics, including duration of reception dropout times
- the spatial distribution of those exposed elements

This thesis work was undertaken to support the charter of the Exposure Statistics Working Group. By constructing a finite difference computer model of the antenna, a design tool was envisioned that would allow engineers to evaluate performance trends and pose "what if" design questions. And most importantly, the computer model would permit performance trade-off studies to be conducted at the system engineering level.

Chapter 2

Model Development

2.1 Characterization of Sea

2.1.1 Linear Theory Ocean Waves

For the purposes of this work, the sea was assumed to be described by linear theory, random, deep-water waves. "Deep water" is defined to exist when $\lambda < 2d$ where d is the water depth. The random aspect of the waves implies that

- the distribution of wave elevations from the calm water level follow a gaussian form, and have zero mean
- the sea statistics obtained from a single location are the same as the statistics obtained from an ensemble of locations (ergodic)
- the sea statistics remain constant with respect to time (steady state process).

Because the last condition is so restrictive, we relax it to allow the statistics to vary slowly with time (weakly steady state process). A summary of the deep water linear theory wave relations is provided in Table 2.1.

Assuming a lower sea spectral energy bound of 0.7 rad/sec, which is reasonable for the range of seas analyzed in this report, this translates into a deep water depth of 252 meters. For depths shallower than about 250 meters, the deep water theory begins to break down, and a depth-dependent treatment of the sea waves must be considered. Referring to the formulas

Quantity	Formula
Wave Number	$k = \frac{2\pi}{\lambda}$
Circular Frequency	$\omega = \frac{2\pi}{T}$
Dispersion Relation	$k = \frac{\omega^2}{g}$
Velocity Potential	$\phi = \frac{ag}{\omega} e^{kz} \sin(kx' - \omega t)$
Surface Displacement	$h = a\cos(kx' - \omega t)$
Radian Frequency	$\omega = \sqrt{gk}$
Phase Velocity	$c = \sqrt{g/k}$
Group Velocity	$c_g = \frac{1}{2}\sqrt{g/k}$
Horizontal Fluid Velocity	$u = a\omega e^{kz} \cos(kx' - \omega t)$
Vertical Fluid Velocity	$w = a\omega e^{kz} \sin(kx' - \omega t)$
Wave Energy Density	$E = \frac{1}{2}\rho g a^2$

Note: x' refers to a stationary x coordinate system.

Table 2.1: Linear Theory Deep Water Wave Relations

in Table 2.1, the wave forms in linear theory can be seen to be sinusoidal. However, simple observation of the sea surface shows that the wave forms display a complicated structure which has random features. This observed behavior can be approximated by adding together a series of sinusoids, each frequency component having the appropriate amplitude and a random phase. As the number of frequency components increases, the approximation approaches the continuous distribution of the actual sea. This discrete method of describing a one dimensional random seaway is presented in equation 2.1

$$h(x', t) = \sum_{i=1}^{N} a_i(\omega) \cos(k_i(\omega)x' - \omega_i t + \phi_i) \tag{2.1}$$

where

$h(x', t)$ is the surface elevation of the sea, referenced to the calm water level

$a_i(\omega)$ is the wave amplitude of each discrete frequency component

$k_i(\omega)$ is the wave number of each frequency component

ω_i is the set of discrete circular frequencies chosen

ϕ_i is the random phase assigned to each frequency component

and the e^{kz} term has been dropped, since evaluation occurs at the sea surface ($z = 0$).

It is fairly straightforward to determine most of the terms on the right hand side of equation 2.1: k_i is determined from the dispersion relation, ϕ_i is a random number with a uniform

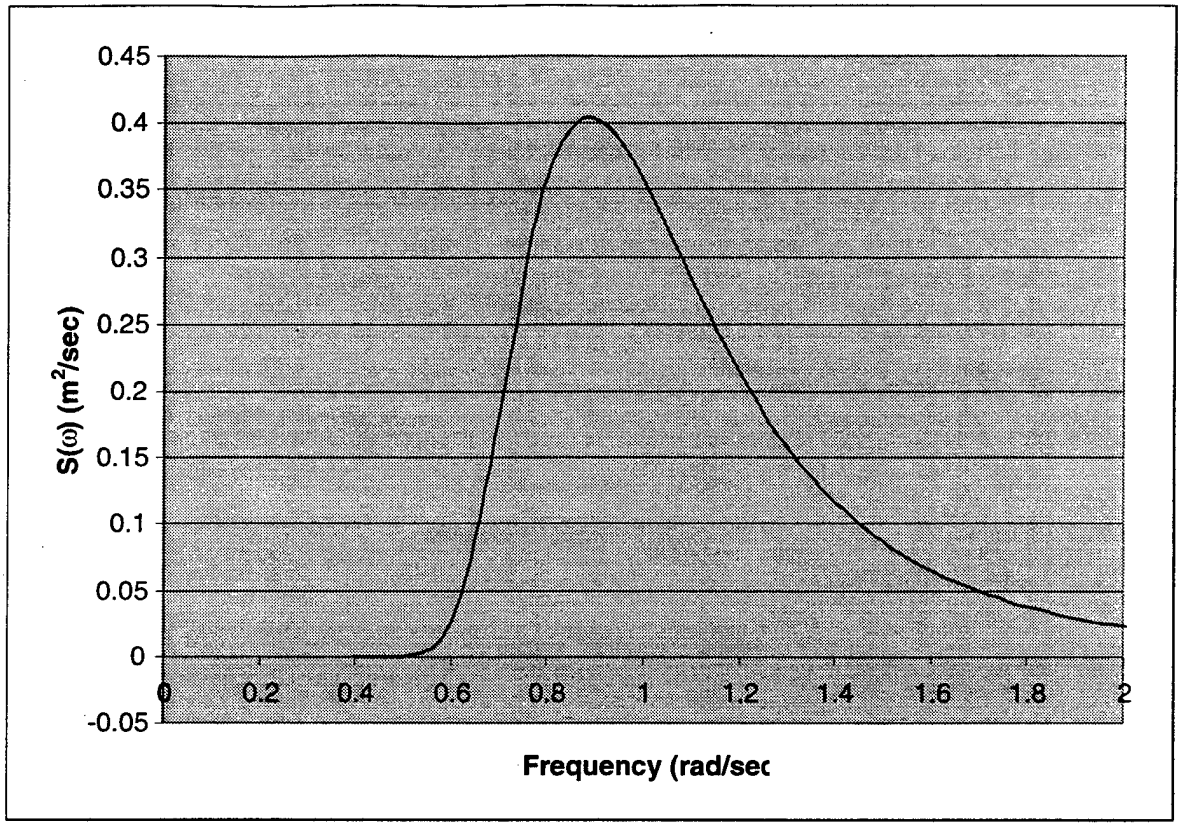

Figure 2-1: Sample Ocean Wave Energy Density Spectrum: $H_s = 2.0$ m

distribution $[0, 2\pi]$. The evaluation of the amplitudes, however, requires some discussion.

We begin by defining the spectral energy density function, $S(\omega)$, which represents the energy of the ocean waves having frequency ω. (See Figure 2-1 for a typical energy density spectrum.) The units of $S(\omega)$ are defined to be in m^2/sec, so that when $S(\omega)$ is integrated with respect to ω, the result is energy in units of m^2. (All that is lacking to give this quantity the normal units of energy is the $\frac{1}{2}\rho g$ term seen in Table 2.1 for the wave energy density.) The spectrum of Figure 2-1 is said to be single-sided, which refers to the fact that the frequencies are constrained to be positive. For a double-sided spectrum (positive and negative frequencies allowed, and the spectrum defined such that $S(\omega) = S(-\omega)$) of equal sea severity, one must divide the spectrum by 2, since for constant sea severity the area under the spectral energy density curve must be

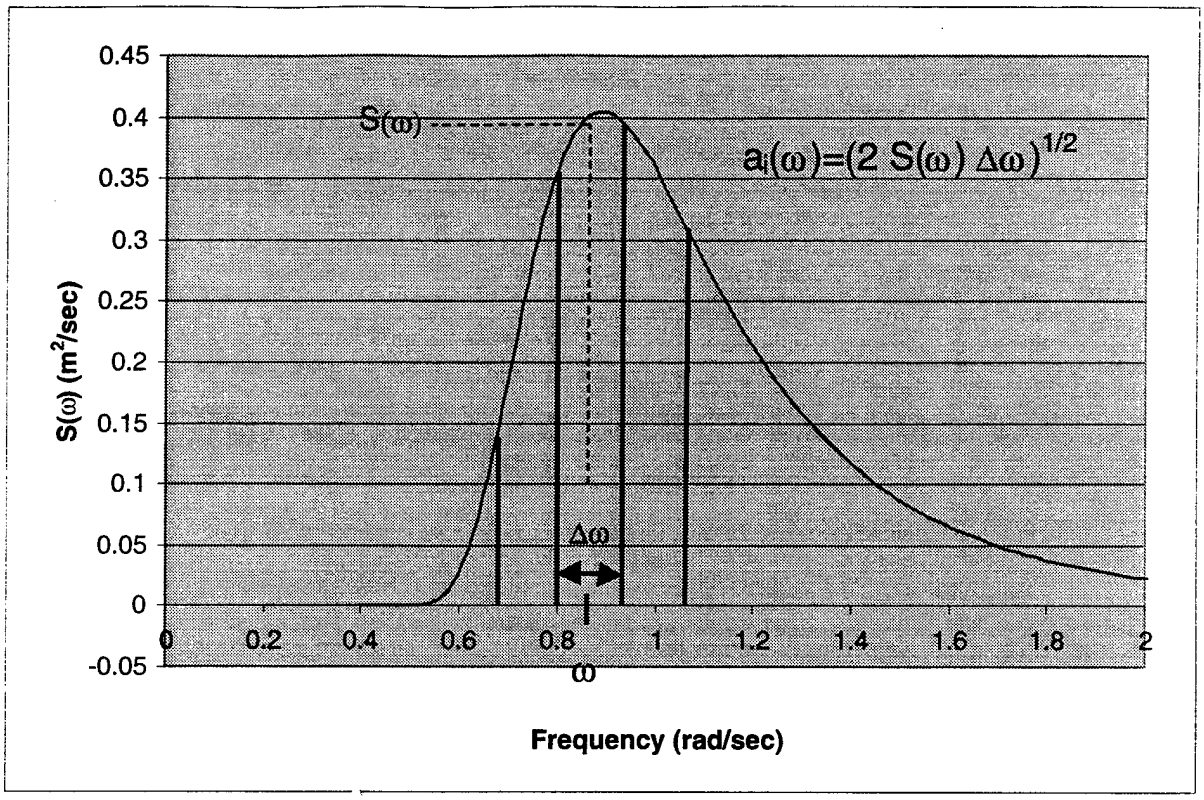

Figure 2-2: Determination of Component Amplitudes $a_i(\omega)$

constant. The amplitudes $a_i(\omega)$ are obtained from Eq. 2.2

$$\frac{1}{2}a_i(\omega)^2 = S(\omega)\Delta\omega \tag{2.2}$$

where

$a_i(\omega)$ is the amplitude of the band of sinusoid waves $\Delta\omega$ with center frequency ω.

Eq. 2.2 is really nothing more than a statement that the square of the wave amplitude is a measure of the average energy of the waves, because both sides of the equation represent energy in units of m^2. A method of obtaining the amplitudes $a_i(\omega)$ is shown in Figure 2-2.

Although $S(\omega)$ has been presented in terms of wave energy content at a given frequency, it can be shown from the Weiner-Kintchine theorem that $S(\omega)$ is related to the wave amplitude record at a fixed location in the ocean. Following Ochi, [2] we define a wave record at a given

location as $x'(t)$. Then the autocorrelation of $x'(t)$ is given by

$$R(\tau) = \lim_{T \to \infty} \frac{1}{2T} \int_{-T}^{T} x'(t)\, x'(t+\tau)\, dt \tag{2.3}$$

and by the Weiner-Kintchine theorem, the spectral energy density function, $S(\omega)$, and the autocorrelation function, $R(\tau)$, form a Fourier transform pair.

$$S(\omega) = \frac{1}{\pi} \int_{-\infty}^{\infty} R(\tau)\, e^{-i\omega\tau} d\tau \tag{2.4}$$

$$R(\tau) = \frac{1}{2} \int_{-\infty}^{\infty} S(\omega)\, e^{i\omega\tau} d\omega \tag{2.5}$$

This method's value lies in its ability to convert observed wave records into spectral energy density functions.

2.1.2 Spectral Energy Density Functional Forms Assumed for the Model

Numerous forms have been proposed by researchers attempting to characterize the sea wave environment [3][4][5][6][7]. The model incorporates the spectral formulation as a subroutine, hence it is completely arbitrary from the model viewpoint how the spectrum is defined. In order to limit the scope of the simulation parameters, yet retain the ability to vary the sea energy form, two wave spectral energy subroutines were developed for the model. Though they may appear very different at first glance, most spectral formulations share the basic framework of Eq. 2.6

$$S(\omega) = \frac{A}{\omega^5} H_s^2 e^{-B/\omega^4} \tag{2.6}$$

where

A, B are constants to be determined

H_s is the significant wave height, which is defined to be the average wave height of the one third highest waves. Sea severity is most commonly given in terms of significant wave height among researchers. However operators (such as U.S. Navy personnel) are frequently more familiar with sea state. (Appendix E provides a conversion between the two systems.) The two spectral formulations chosen for the model are the Bretschneider two parameter spectrum, and the Ochi six parameter spectrum, given in Eqs. 2.7 and 2.8 respectively [2].

$$S(\omega) = \frac{1.25}{4}\frac{\omega_m^4}{\omega^5}H_s^2 e^{-1.25(\omega_m/\omega)^4} \tag{2.7}$$

$$S(\omega) = \frac{1}{4}\sum_{j=1}^{2}\frac{(\frac{4\lambda_j+1}{4}\omega_{mj}^4)^{\lambda_j}}{\Gamma(\lambda_j)}\frac{H_{sj}^2}{\omega^{4\lambda_j+1}}e^{-(\frac{4\lambda_j+1}{4})(\omega_{mj}/\omega)^4} \tag{2.8}$$

Bretschneider Two Parameter Spectrum

The two parameters of the Bretschneider spectrum (Eq. 2.7) are significant wave height, H_s, and modal frequency, ω_m. Modal frequency is that frequency at which $S(\omega)$ reaches its maximum value, and significant wave height is as previously defined. For the special case of a fully developed sea (also referred to as a fully arisen sea), i.e. one in which the wind imparts energy to the waves at a rate equal to that at which viscous damping dissipates their energy and wave-wave interactions transmit energy from one frequency to another; a relationship exists between ω_m and H_s. Designating this modal frequency as $\omega_{m_{FA}}$, we have

$$\omega_{m_{FA}} = 0.4\sqrt{\frac{g}{H_s}} \tag{2.9}$$

which establishes the energy equilibrium characteristic of a fully arisen sea. The two requirements for a fully arisen sea are

- sufficient fetch (i.e. the distance over which the wind is blowing over the water.)
- sufficient duration (i.e. the length of time the wind has been blowing.)

If the fetch or duration are insufficient, the modal frequency will be greater than that given by Eq. 2.9; if the winds are subsiding, the modal frequency will be less than that given by Eq. 2.9. This is best understood by considering the mechanism by which waves are generated. The wind causes ripples (capillary waves) on the sea surface, which is a short wavelength, high frequency phenomenon. Thus as a storm is building, wave energy input occurs at high frequency, and the energy gradually is transferred through wave-wave interactions to lower frequencies. Likewise, as a storm is subsiding, the high frequency waves attenuate most rapidly due to viscous effects, and the result is a skewing of the spectral energy toward lower frequencies. By

Parameter	Value
H_{s1}	$0.84H_s$
H_{s2}	$0.54H_s$
ω_{m1}	$0.70e^{-0.046H_s}$
ω_{m2}	$1.15e^{-0.039H_s}$
λ_1	3.00
λ_2	$1.54e^{-0.062H_s}$

Table 2.2: Ochi Six Parameter Spectrum: Most Probable Values in Terms of Hs

introducing a term we will call the development Dev, we can quantify the degree of sea arousal as given in Eq. 2.10.

$$\omega_m = Dev \cdot \omega_{m_{FA}} \tag{2.10}$$

Using this convention, values of $Dev < 1.0$ correspond to a decaying sea, and values of $Dev > 1.0$ correspond to a building sea. Figures 2-3 and 2-4 show representative plots of $S(\omega)$ as development and significant wave height, respectively, are varied. Note that in Fig. 2-3, that while changing the development shifts the location of peak spectral energy density, it keeps the area under the curve (and thus the total energy) constant.

Ochi Six Parameter Spectrum

The Ochi six parameter spectrum is a generalization of the Bretschneider two parameter spectrum in two respects:

- two spectral peaks are present, each with their own modal frequency and significant wave height, and their contributions add together
- a shape factor, λ, can be applied to each spectral peak to skew the curve right or left, independent of the significant wave height or modal frequency.

In the form given in Eq. 2.8, each parameter is an independent variable. However, by analyzing 800 wave spectra from the North Atlantic [2], one can obtain a relationship for the six parameters in terms of the measured significant wave height. Ochi reports the results of this analysis for a family of spectra having a 95% confidence, however the results given in Table 2.2 represent a single "most probable" spectrum [2]. The model implemented the most probable

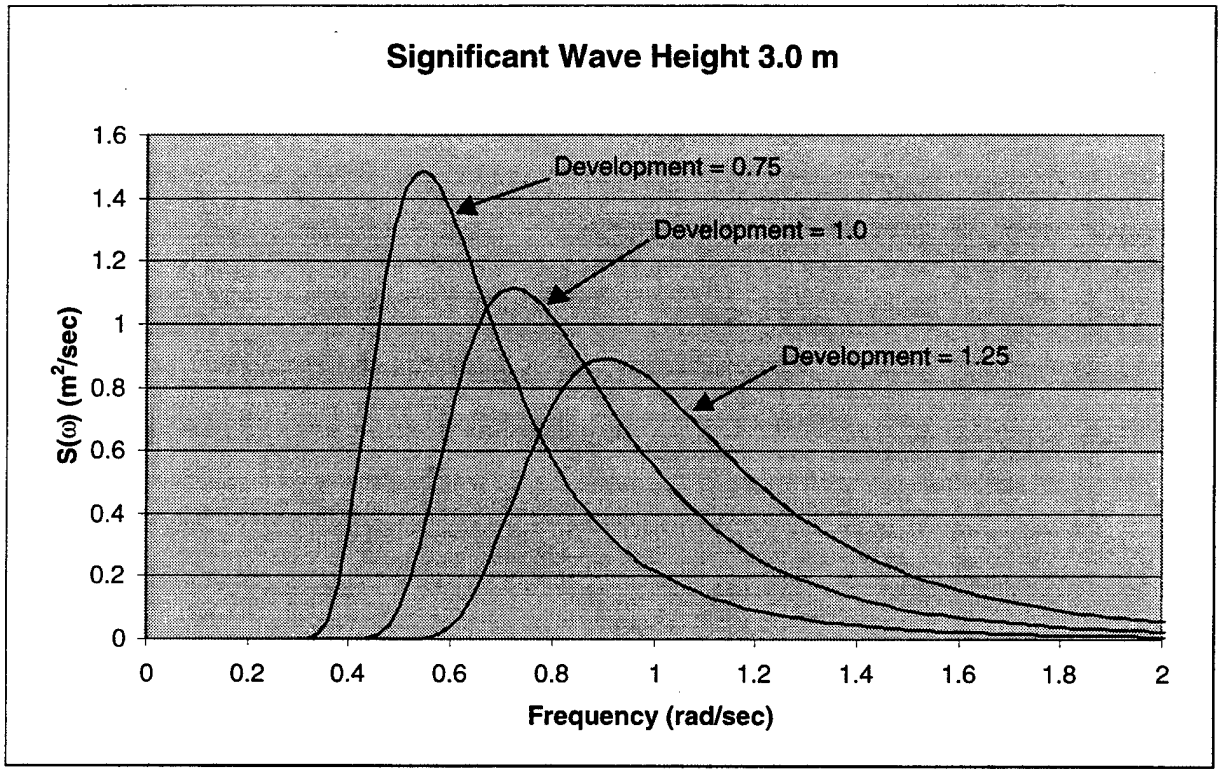

Figure 2-3: Bretschneider $S(\omega)$ for Varying Degrees of Development

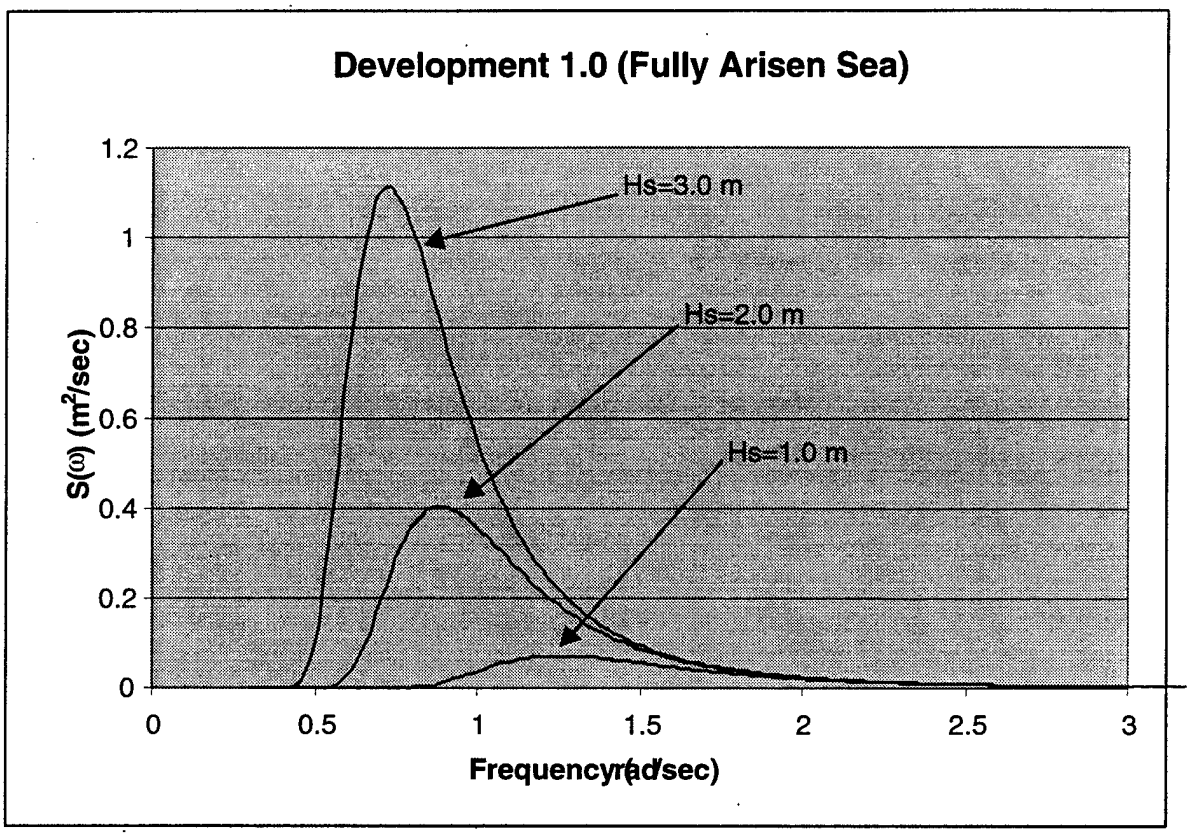

Figure 2-4: Bretschneider $S(\omega)$ for Varying Sea Severity, H_s

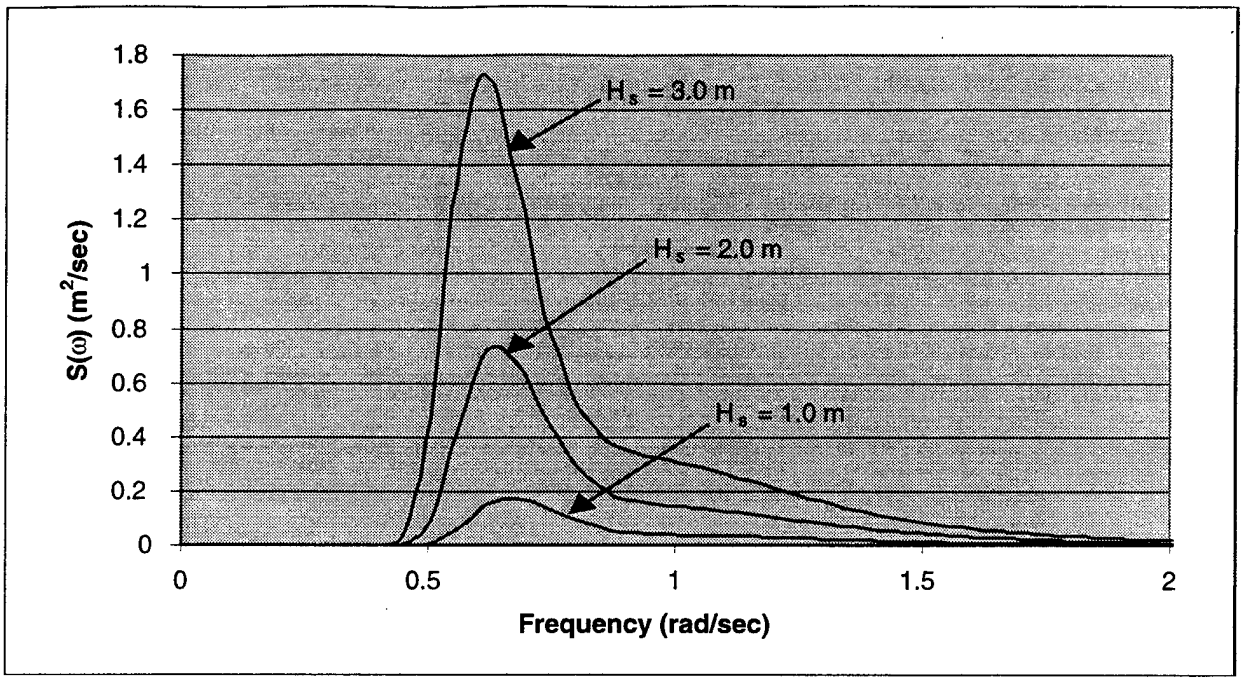

Figure 2-5: Ochi Six Parameter "Most Probable" Spectrum

form for obtaining the six parameters of the Ochi spectrum. A sample plot of the Ochi most probable spectrum, showing its characteristic bimodal shape, is provided in Figure 2-5.

2.2 Coordinate System Description

The coordinate system adopted for the model is a two-dimensional (x-z) system whose origin translates in the x direction at the antenna tow speed U. For the case of head seas, U is defined to be negative and the waves travel in the positive x direction. Conversely, for the stern sea case U is positive and the waves again travel in the positive x direction. Figures 2-6 and 2-7 depict the coordinate system employed and the basic antenna configuration for both the head and stern sea cases. The equations listed in Table 2.1 apply to a stationary coordinate system. The transformation to a moving coordinate system employs the simple relationship

$$x' = x + Ut \tag{2.11}$$

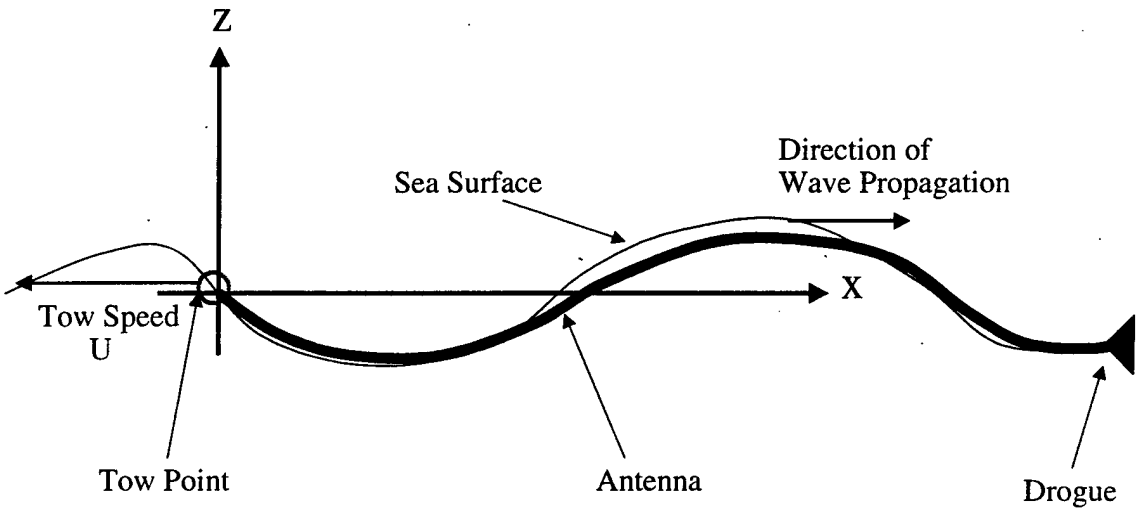

Figure 2-6: Coordinate System: Head Seas

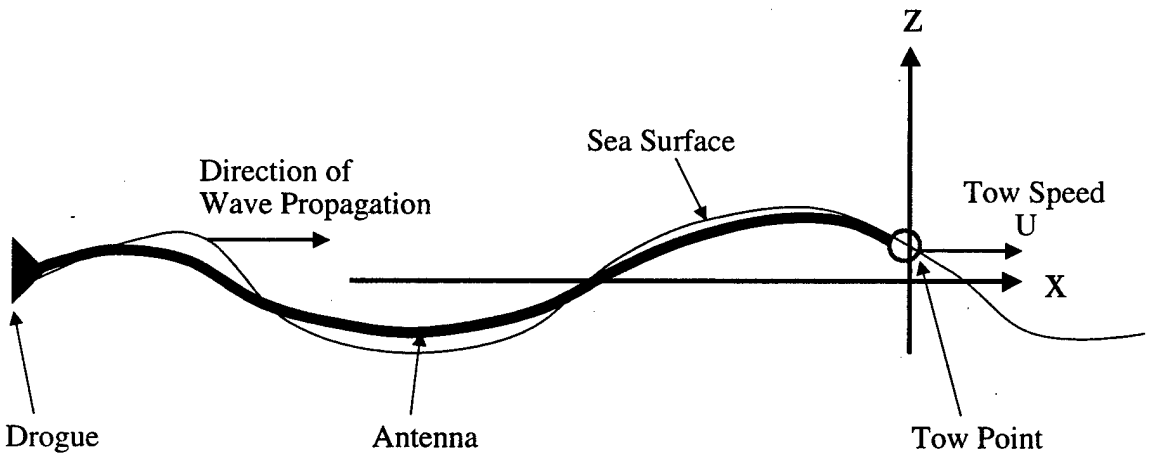

Figure 2-7: Coordinate System: Stern Seas

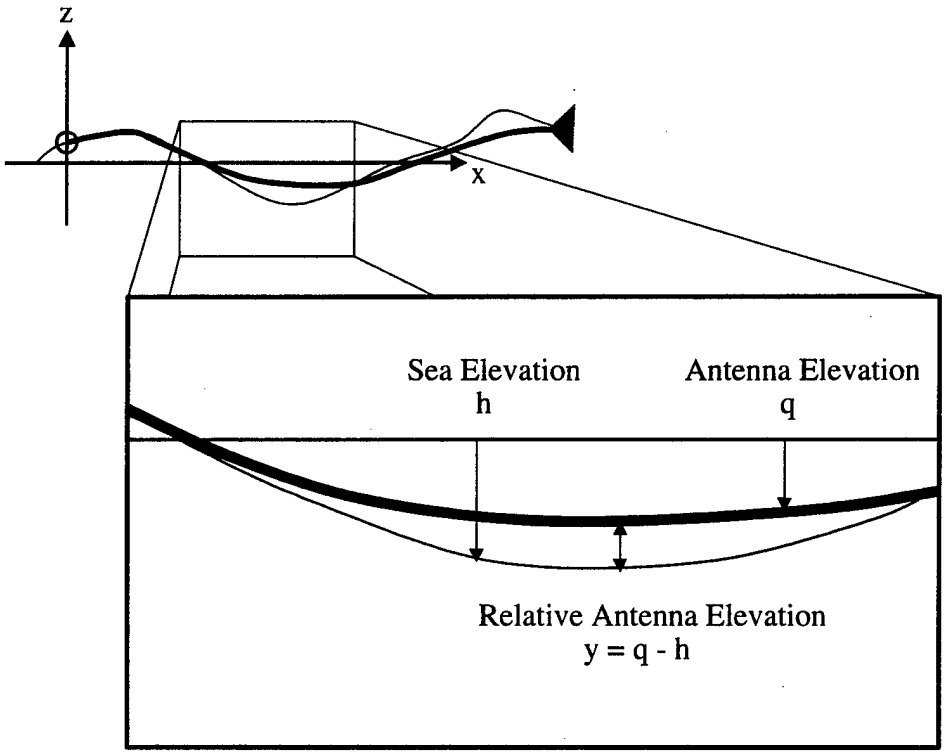

Figure 2-8: Closeup Showing Key Antenna Position Variables

where

x' is the earth-fixed (stationary) coordinate system

x is the moving coordinate system whose origin translates with velocity U (as shown in Figure 2-6 and 2-7).

2.3 Forces Acting on Antenna

The vertical forces acting on the antenna are given in the right hand side of Eq. 2.12

$$m\frac{dv}{dt} = T(x,t)\frac{\partial^2 q}{\partial x^2} + C_D\,(w-v)|w-v| + b(x,t) + C_{MA}\,\rho_{water}\,\pi r^2\frac{dw}{dt} + EI\frac{\partial^4 q}{\partial x^4} \qquad (2.12)$$

where

m is the mass per unit length of the antenna, assumed uniform

v is antenna vertical velocity (i.e. $\frac{dq}{dt}$)

$T(x,t)$ is the tension along the length of the antenna, arising from skin frictional drag between the submerged portion of the antenna and the water

q is the z coordinate of the antenna central axis

C_D is the normal drag coefficient of a cylindrical antenna section as it moves in the z direction through the water

w is the vertical fluid velocity

$b(x,t)$ is the buoyancy force, which is the resultant of its weight (downward force) and water displaced (upward force)

C_{MA} is the coefficient of added mass for a cylindrical section in a flow field normal to its long axis

ρ_{water} is the density of water (for seawater of 15° C, $\rho_{water} = 1025.9$ kg/m^3)

r is the antenna radius

EI is the product of the antenna cross sectional modulus of elasticity and area moment of inertia (thus a measure of lateral stiffness).

Thus, the first term on the right hand side of Eq. 2.12 represents a restoring force characteristic of a string displaced from its (taut) equilibrium condition. The tension in the antenna is calculated from the time varying wetted surface area along the length of the antenna. A

tangential drag coefficient of $C_T = 0.0035$ was used [8]. (Reynold's numbers varied from 32,940 to 494,130 for speed/diameter combinations of 3 knots/1 inch to 9 knots/5 inches, respectively.) The second term represents the normal drag force a cylindrical element would experience as it is moved through the fluid with its long axis perpendicular to the direction of motion. A value of $C_D = 1.0$ was used (assumes infinite fluid domain). The fourth term represents the added mass effect experienced by a cylindrical object as the fluid around is accelerating normal to the long axis of the cylinder. A value of $C_{MA} = 2.0$ was selected (assumes infinite fluid domain), consistent with standard fluid dynamic texts [9]. The final term represents the restoring force due to the stiffness of the material, and its distribution with respect to the neutral axis. At this preliminary stage of the antenna design, a material similar to Tygon® tubing is planned for the outer antenna housing. At a nominal design of 3 inch outer diameter, 0.25 inch wall thickness, and modulus of elasticity $E = 1.5 \cdot 10^8$ Pa, we have a relatively flexible antenna of about $EI = 300$ Pa m^4.

It is recognized that some of these forces have been approximated, namely in that the values quoted above are for C_D and C_{MA} in an infinite fluid domain. The antenna operates in close proximity to the free surface, and occasionally portions rise completely above the surface of the water. A rigorous treatment of the behavior of C_D and C_{MA} near the free surface was not attempted. Rather, a straightforward linear approximation was employed which varied the coefficients C_D and C_{MA} from their infinite fluid domain values when the antenna axis was at a depth of r (i.e. just submerged), to a value of zero when the antenna axis was at a height of r (i.e. just breaking out of the water). This dependence of C_D and C_{MA} on relative antenna depth y is shown in Eqs. 2.13 and 2.14.

$$C_D(y) = C_{D_{Infinite}}(-\frac{y}{2r} + \frac{1}{2}) \tag{2.13}$$

$$C_{MA}(y) = C_{MA_{Infinite}}(-\frac{y}{2r} + \frac{1}{2}) \tag{2.14}$$

2.4 Discretization

The antenna, of length L, is subdivided first into lengths of the physical radio antenna elements. These antenna elements, designed at Lincoln Laboratory, are called "jelly roll" antennas because

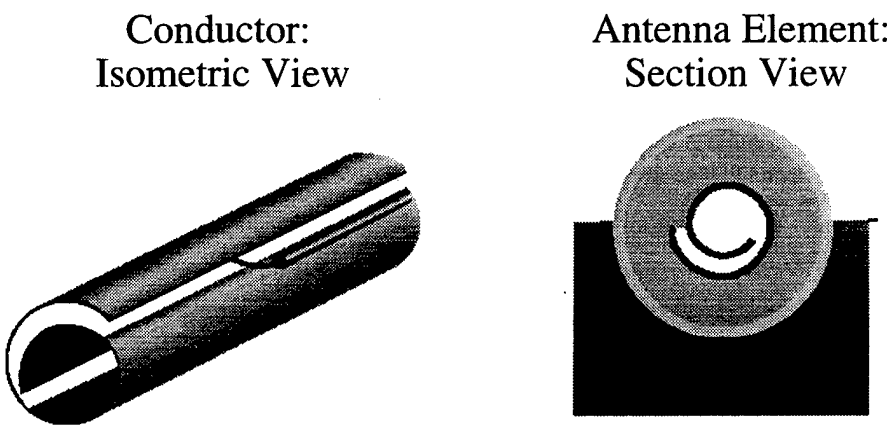

Figure 2-9: "Jelly Roll" Antenna Element Construction [12]

they are a conducting sheet rolled up about $1\frac{1}{2}$ times. (See Figure 2-9 for the construction of an antenna element.) The element length is designated L_{elem}. This first level of subdivision is not only logical, but necessary for the exposure statistics calculated by the model. As it turns out, this type of antenna element performs well as long as it has some small amount (e.g. 1 mm) of its outer housing diameter exposed along its entire length. But if the element becomes covered by even a small amount of water at any point along its length, antenna performance drops dramatically. Thus it is necessary to monitor numerous points within each element to determine whether a given element is exposed or not. This leads to the final level of antenna subdivision: each element is meshed into some integer number M of sections with length Δs. The subdivision process is shown in Figure 2-10.

An interesting feature of the program version which calculates the sea elevation and fluid velocities by Fast Fourier Transforms (FFTs) is that the frequency meshing ($\Delta\omega$) of the spectral energy density function $S(\omega)$, is now related to the spatial meshing (Δx) of the sea, and thus the spatial meshing of the antenna (Δs). This means that there is an extra constraint to consider in selecting the finest antenna mesh size Δs; or conversely, given a mesh size Δs, constraints

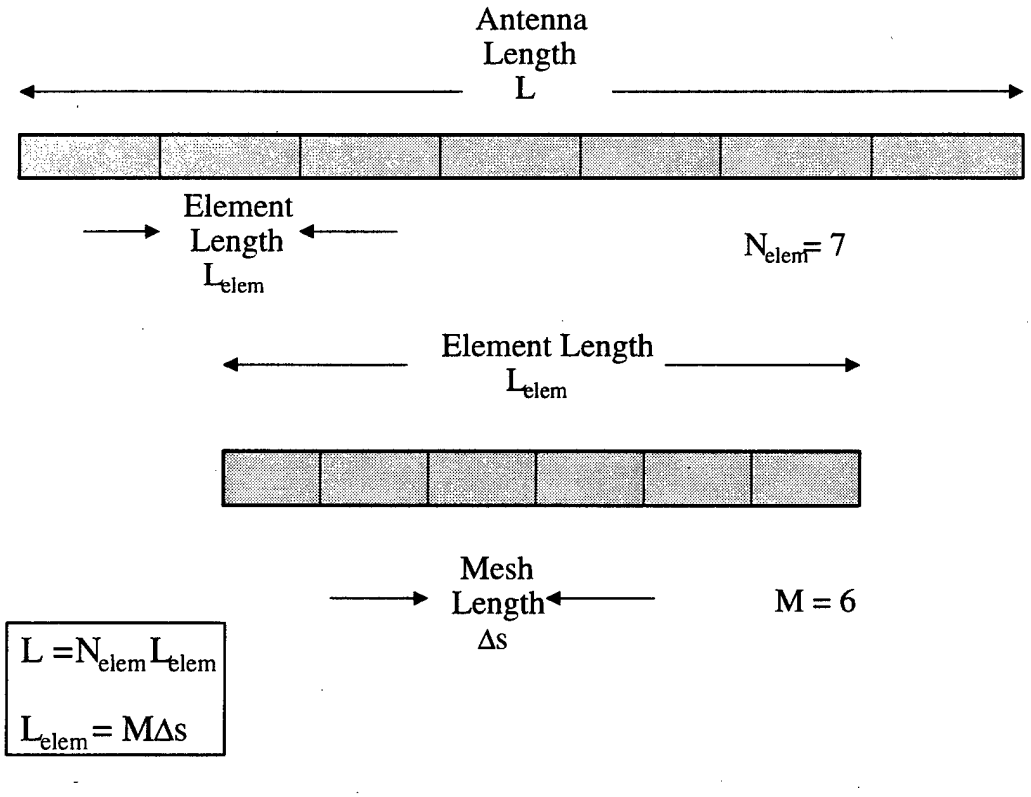

Figure 2-10: Antenna Subdivsion

are imposed on the $\Delta\omega$ meshing of the spectral energy density function $S(\omega)$. Some freedom is regained if one decouples the length of the antenna and the length of the sea simulated. This decoupling is implemented in the model, so that for a typical run the antenna may be 25 m long with a mesh size of 0.0625 m, while the length of sea modeled is 512 m long with a mesh size of 0.0625 m. The key point is that the mesh length between the antenna (Δs) and the sea (Δx) must match.

2.5 Computational Method

2.5.1 Sea Domain Properties

The sea domain variables of interest are

- sea elevation, h
- fluid horizontal velocity, u
- fluid vertical velocity, w.

Two methods were employed in arriving at the sea domain properties, each with certain advantages and disadvantages. The first method will be called Sine Wave Superposition (SWS), and the second method will be called Fast Fourier Transform (FFT). The source code for both of these computer programs can be found in reference [10].

Sine Wave Superposition (SWS) Method

As previously mentioned in Eq. 2.1, the sea elevation can be obtained by a superposition of sine waves having random phase and amplitude prescribed by Eq. 2.2. In like manner the fluid velocities can be calculated by the superposition method. The formulas for h, u and w in an earth-fixed reference frame are provided in Eqs. 2.15 - 2.17.

$$h(x',t) = \sum_{i=1}^{N} a_i(\omega)\cos(k_i(\omega)\,x' - \omega_i t + \phi_i) \tag{2.15}$$

$$u(x',t) = \sum_{i=1}^{N} a_i(\omega)\;\omega\cos(k_i(\omega)\,x' - \omega_i t + \phi_i) \tag{2.16}$$

$$w(x',t) = \sum_{i=1}^{N} a_i(\omega)\ \omega \sin(k_i(\omega)\, x' - \omega_i t + \phi_i) \tag{2.17}$$

By invoking the coordinate transformation and the dispersion relation (Eq. 2.11 and Table 2.1, respectively), one arrives at the forms appropriate to the coordinate system moving with the antenna. These are presented in Eqs. 2.18 - 2.20.

$$h(x,t) = \sum_{i=1}^{N} a_i(\omega) \cos\left[k_i(\omega)\, x - (\omega_i - \frac{\omega_i^2 U}{g})t + \phi_i\right] \tag{2.18}$$

$$u(x,t) = \sum_{i=1}^{N} a_i(\omega)\ \omega \cos\left[k_i(\omega)\, x - (\omega_i - \frac{\omega_i^2 U}{g})t + \phi_i\right] \tag{2.19}$$

$$w(x,t) = \sum_{i=1}^{N} a_i(\omega)\ \omega \sin\left[k_i(\omega)\, x - (\omega_i - \frac{\omega_i^2 U}{g})t + \phi_i\right] \tag{2.20}$$

The spectral energy density function $S(\omega)$ used in this formulation was a single sided one. The advantages of the SWS method are

- simplicity in coding fluid property subroutines
- good resolution for $S(\omega)$ at lower frequencies, where most of the wave energy resides
- frequency meshing ($\Delta\omega$) is unrelated to the spatial meshing (Δx), allowing both antenna element length and wave energy frequency resolution to be arbitrarily chosen.

Fast Fourier Transform (FFT) Method

This method takes advantage of the fact that Eqs. 2.15 - 2.17 are a Fourier series, and thus the functions h, u,and w are the inverse Fourier transform of some expression. Since the calculations to determine the sea domain properties occur at a fixed point in time, the transform variables are not ω and t, rather they become b and x. Table 2.3 summarizes the analogous relationships between the time-frequency domains and the space-spatial frequency domains. (The first two lines may be taken as definitions; the last line utilizes the dispersion relation.) Because the FFT algorithm used for the model assumed the presence of both positive and negative frequency components, it was necessary to use a two sided spectrum for this method. In order to retain the same amount of energy (i.e. area under the spectral energy density curve) as the transition

Time-Frequency Domain	Space-Spatial Frequency Domain
$f = 1/T$	$b = 1/L$
$\omega = 2\pi f$	$k = 2\pi b$
$k = (2\pi f)^2/g$	$\omega = \sqrt{2\pi g b}$

Table 2.3: Comparison of Fourier Transform Domain Relationships

from one-sided to two-sided spectra is made, it is necessary that the formula for the component amplitudes be adjusted from that given in Eq. 2.2. In addition, it is convenient to incorporate the random phase ϕ_i into a complex component amplitude c_i. With these changes in mind, the formulas providing the sea domain properties are given in Eqs. 2.21 - 2.25.

$$h(x) = \mathrm{Re}\left\{\sum_{i=1}^{N} c_i(b_i) \exp\left[i(2\pi b_i x + (2\pi b_i U - \sqrt{2\pi g b_i})\, t)\right]\right\} \tag{2.21}$$

$$u(x) = \mathrm{Re}\left\{\sum_{i=1}^{N} c_i(b_i)\sqrt{2\pi g b_i} \exp\left[i(2\pi b_i x + (2\pi b_i U - \sqrt{2\pi g b_i})\, t)\right]\right\} \tag{2.22}$$

$$w(x) = \mathrm{Re}\left\{\sum_{i=1}^{N} -i\, c_i(b_i)\, \sqrt{2\pi g b_i} \exp\left[i(2\pi b_i x + (2\pi b_i U - \sqrt{2\pi g b_i})\, t)\right]\right\} \tag{2.23}$$

$$\mathrm{Re}\{c_i(b_i)\} = \sqrt{\frac{1}{2} S(b_i)\, \Delta b}\ \cos(\phi_i) \tag{2.24}$$

$$\mathrm{Im}\{c_i(b_i)\} = \sqrt{\frac{1}{2} S(b_i)\, \Delta b}\ \sin(\phi_i) \tag{2.25}$$

Then the Fourier transform pairs become

$$H(b) \Leftrightarrow h(x) \tag{2.26}$$

$$\sqrt{2\pi g b_i}\, H(b) \Leftrightarrow u(x) \tag{2.27}$$

$$-i\sqrt{2\pi g b_i}\, H(b) \Leftrightarrow w(x) \tag{2.28}$$

where

$$H(b) = \sum_{i=1}^{N} c_i(b) \exp\left[it\left(2\pi b_i U - \sqrt{2\pi g b_i}\right)\right] \tag{2.29}$$

and

$$H(b) \Leftrightarrow h(x) \tag{2.30}$$

is defined to mean

$$H(b) = \sum_{i=1}^{N} h(x) \exp(-i2\pi bx) \tag{2.31}$$

$$h(x) = \frac{1}{2\pi} \sum_{i=1}^{N} H(b) \exp(i2\pi bx) \tag{2.32}$$

By setting the complex component amplitudes c_i to obey the relation

$$c_i(b_i) = \overline{c_i(-b_i)} \tag{2.33}$$

that is, the positive frequency components are the complex conjugates of the negative frequency components, then the imaginary parts of Eqs. 2.21-2.23 are zero, and the Re{ } can be dropped from the equations. When converting between expressing the spectral energy density function as a function of ω to another variable, such as b, the basic relations of Eqs. 2.34 and 2.35 are useful.

$$S(\omega)\, d\omega = S(b)\, db \tag{2.34}$$

$$S(b) = S(\omega) \frac{d\omega}{db} \tag{2.35}$$

An important feature of the FFT method is the linkage of the spatial frequency domain meshing (Δb), and the sea spatial meshing (Δx). As previously mentioned, the key to the FFT method is to make the antenna spatial meshing, Δs, match the sea domain spatial meshing, Δx. This is accomplished by using the relations given in Eqs. 2.36 - 2.39, and ensuring that the sea Δx equals the desired antenna Δs.

$$\Delta b = \frac{1}{L_{sea}} = b_{\min} \tag{2.36}$$

$$b_{\max} = \frac{N_{sea} \Delta b}{2} = \frac{N_{sea}}{2L_{sea}} = \frac{1}{2\,\Delta x} \tag{2.37}$$

$$\omega_{\min} = \sqrt{2\pi g b_{\min}} \tag{2.38}$$

$$\omega_{\max} = \sqrt{2\pi g b_{\max}} \tag{2.39}$$

The primary advantage of the FFT method is computational speed. The FFT method

	Frequency, ω_i	
Component	SWS Method	FFT Method
1	0.347	0.347
2	0.381	0.491
3	0.414	0.601
4	0.448	0.694
5	0.482	0.776
6	0.515	0.850
7	0.549	0.918
8	0.583	0.981
9	0.617	1.041
10	0.650	1.097

Notes:
1. FFT case: $\omega \in [0.347, 22.2]$ with 4096 frequency components
2. SWS case: $\omega \in [0.347, 24.0]$ with 700 frequency components

Table 2.4: Comparison of Frequency Resolution for the SWS and FFT Methods

executes approximately 10 times faster than the SWS version. A further increase in execution speed is accomplished by not computing the FFT every time step, Δt. Rather, the sea data (h, u, w) is computed at $n\Delta t$ intervals, and linearly interpolated in between. The integer n is determined by the computer model using the highest sea energy frequency component, $\omega_{\max}$, and the initial estimate of the time step, Δt. This ensures that the linearly interpolated sea evolves in a smooth and continuous fashion.

Its disadvantage is that it has poorer low frequency resolution of the sea wave energy than its SWS counterpart. This is demonstrated by a typical run case in Table 2.4 where the lowest 10 frequencies defined are listed for both methods.As one can readily calculate from integrating Eq. 2.7 with respect to ω, for a sea severity of 2.0m significant wave height, 67.7% of the sea wave energy lies below a frequency of 1.097 rad/sec. Thus the FFT method suffers in that it places most of the frequency components at high frequencies, where little of the wave energy resides. This undesirable result is a consequence of choosing a b space meshing with constant Δb, which is necessary to compute FFT's in the b and x domains. (Constant Δb meshing produces a non-constant $\Delta\omega$ meshing with $\Delta\omega_i = \sqrt{2\pi g b_{\min}}\left(\sqrt{i} - \sqrt{i-1}\right)$.)

2.5.2 Integration Method

The time marching integration method implemented is an explicit forward Euler scheme. Such schemes are characterized by using information at time t to calculate functions at time $t + \Delta t$. A simple example of how the forward Euler method is used is given below.

Solve

$$\frac{du}{dt} = u^2 \tag{2.40}$$

$$u(0) = 1 \tag{2.41}$$

The time derivative is approximated using the Euler method as

$$\left.\frac{du}{dt}\right|_{t=t^n} = \frac{U^{n+1} - U^n}{t^{n+1} - t^n} \tag{2.42}$$

which for constant time step Δt becomes

$$\left.\frac{du}{dt}\right|_{t=t^n} = \frac{U^{n+1} - U^n}{\Delta t} \tag{2.43}$$

having adopted the notation of Celia and Gray [11], where

$$U^n \equiv u(t^n) \tag{2.44a}$$

and t^n is the n^{th} time step. Then the solution proceeds step by step, beginning with the initial value of u given in Eq. 2.41

$$\left.\frac{du}{dt}\right|_{t=0} = u(0)^2 = 1 \tag{2.45}$$

then solving Eq. 2.43 for U^{n+1} we obtain

$$U^1 = U^0 + \Delta t \left.\frac{du}{dt}\right|_{t=0} \tag{2.46}$$

With the value of u now known at time t (U^1), we can calculate

$$\left.\frac{du}{dt}\right|_{t=1} = \left(U^1\right)^2 \tag{2.47}$$

and

$$U^2 = \dot{U}^1 + \Delta t \left.\frac{du}{dt}\right|_{t=t^1} \tag{2.48}$$

In like manner, we move forward in time to calculate any desired U^n.

Spatial derivatives ($\frac{d^n q}{dx^n}$) alternate between forward centered and backward centered as the derivative order n increases, accomplishing a space centered scheme. Thus the algorithm can be classified as a forward time, centered space (FTCS) method. For many designs considered, the antenna was approximated as a flexible string of negligible stiffness. With this in mind, Eq. 2.12 becomes a string vibration type equation with damping. As such the Courant condition [11, p. 231] becomes a useful starting point in selecting a time step size. The Courant condition, Eq. 2.49

$$\frac{c\,\Delta t}{\Delta x} \leq 1 \tag{2.49}$$

where

c is the speed at which waves (i.e., disturbances) propagate down the antenna

Δt is the time step size

Δx is the antenna spatial mesh size

is used to calculate an initial time increment based on the string wave velocity given by Eq. 2.50.

$$c = \sqrt{\frac{T}{\rho}} \tag{2.50}$$

In Eq. 2.50

T is the string tension, and

ρ is the linear string density.

Because the tension varies with time, and the maximum tension varies with sea severity (due to tangential drag associated with the square of local fluid velocities), the calm water tension is used in Eq. 2.50 to form an initial estimate of the time step. Then by multiplying the calm water time step by a safety factor, a time step appropriate to the sea severity is arrived at. (For a 3.0 m significant wave height, this safety factor is typically set to 0.25) When the antenna is modeled as having stiffness, the velocity at which disturbances propagate down the antenna is now frequency dependent, and the above implementation of the Courant condition no longer applies. Numerical experimentation was used to determine the safety factor which

produced an acceptable time step size.

2.5.3 Boundary Conditions

The boundary conditions imposed on the antenna endpoints are given in Eqs.

$$q(0) = h(0) \tag{2.51}$$

$$q(L) = h(L) \tag{2.52}$$

That is, the antenna follows the sea surface at its endpoints. This is envisioned to be accomplished at the trailing end by a drogue having positive buoyancy, and at the tow point by one of several options. These options include

- a lifting body
- a surface following buoy
- a leader of positive buoyancy
- some combination of the above features.

The problem pertaining to the antenna leader (that portion from the submarine tow point up to the surface) is being studied by another graduate student at MIT, and will not be addressed in this thesis.

2.5.4 Initial Conditions

The antenna simulation begins at $t = 0$ with

$$q(x) = h(x) \tag{2.53}$$

$$\frac{dq(x)}{dt} = \frac{dh(x)}{dt} \tag{2.54}$$

that is, the antenna is placed at the sea surface, and given an initial vertical velocity matching that of the sea surface.

Chapter 3

Verification of Model Seas

3.1 Significant Wave Height

The random seaway was constructed by the SWS and FFT methods, as described in Sections 2.5.1and 2.5.1. By running the sea generation subroutines, and sampling the wave amplitude record, one can determine the significant wave height of the sample. This can then be compared to the significant wave height which was originally specified. From Ochi[2] we have that the sample's significant wave height can be found by Eqs. 3.1 and 3.2,

$$\widehat{\sigma}^2 = \frac{1}{n-1} \cdot \sum_{i=1}^{N} h_i^2 \tag{3.1}$$

$$\widehat{H}_s = 4.01 \cdot \widehat{\sigma} \tag{3.2}$$

where

h_i is the sampled wave amplitude, measured from the calm water level

$\widehat{\sigma}$ is the standard deviation of the sampled wave amplitudes

$\widehat{H}_s$ is the measured significant wave height of the sample.

(The " $\widehat{\ }$ " symbol denotes that the quantity is computed from a sample, and therefore may deviate somewhat from the theoretical value.)

A sea severity of 3.0 m significant wave height was simulated by both the SWS and the FFT methods. Twelve wave amplitude records were analyzed by sampling the seas at 8.0 m intervals. The results are summarized in Table 3.1. Good agreement to the specified significant

	FFT			SWS		
Sample	Mean(h_i) (m)	$\widehat{\sigma}$ (m)	$\widehat{H}_s$ (m)	Mean(h_i) (m)	$\widehat{\sigma}$ (m)	$\widehat{H}_s$ (m)
1	-0.0008	0.7535	3.0214	-0.0005	0.7463	2.9928
2	0.0002	0.7512	3.0124	0.0002	0.7498	3.0068
3	-0.0003	0.7490	3.0037	-0.0006	0.7464	2.9932
4	-0.0003	0.7481	2.9997	-0.0006	0.7494	3.0051
5	0.0006	0.7511	3.0119	-0.0010	0.7475	2.9976
6	0.0010	0.7516	3.0140	0.0010	0.7484	3.0009
7	0.0001	0.7504	3.0092	0.0000	0.7503	3.0088
8	-0.0001	0.7509	3.0112	-0.0002	0.7501	3.0081
9	-0.0006	0.7490	3.0033	0.0018	0.7483	3.0007
10	-0.0004	0.7489	3.0032	-0.0011	0.7525	3.0170
11	0.0002	0.7492	3.0044	0.0002	0.7479	2.9991
12	0.0002	0.7500	3.0075	-0.0005	0.7505	3.0095
Std. Dev.'s:	0.0005	0.0015	0.0061	0.0008	0.0018	0.0072
Averages:	0.0000	0.7502	**3.0085**	-0.0001	0.7489	**3.0033**

Table 3.1: Simulated Significant Wave Heights for a Specified Sea Severity of 3.0 m

wave height is achieved, with an average overshoot in $\widehat{H}_s$ of 0.28% and 0.11% for the FFT and SWS methods, respectively.

3.2 Wave Period

Determination of the wave period (or wavelength, frequency, etc.) becomes difficult for a random seaway, where wave shapes and heights are constantly evolving. However, it is quite necessary to verify the wave period, because it is possible to correctly model the sea's significant wave height, but incorrectly model the wave period (which the research inadvertently proved). The method used to verify the wave period invoked the superposition principle: the sea waves generated by both methods are ultimately a superposition of individual sine waves, thus the verification of wave period was restricted to seas represented by a single harmonic wave. An important aspect of this process is to verify that the antenna sees the correct "encounter frequency," i.e. an effective change of the wave frequency as the antenna is towed in a seaway. The encounter frequency, ω_e, is given by

$$\omega_e = \omega_0 - \frac{\omega_0^2 \cdot U}{g} \tag{3.3}$$

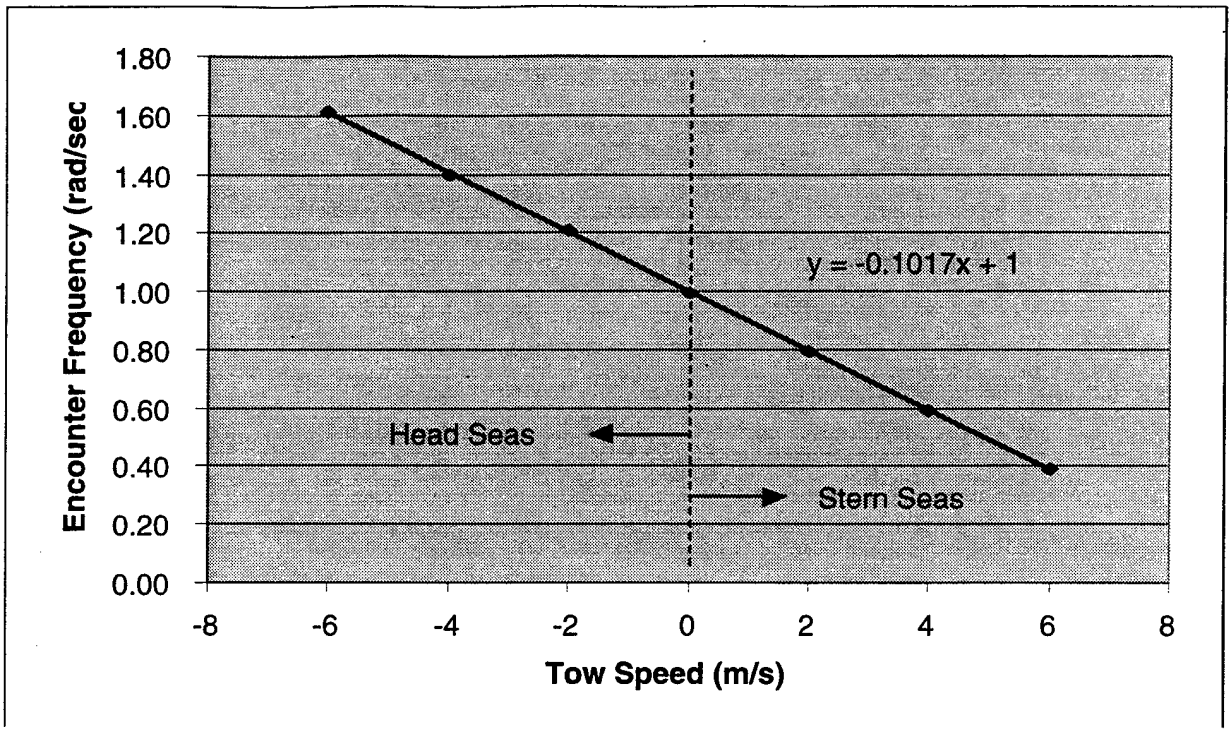

Figure 3-1: Variation of Encounter Frequency vs. Tow Speed

where

ω_0 is the wave frequency in a stationary coordinate system

U is the antenna tow speed

g is the acceleration due to gravity.

Thus for towing into head seas (U is negative), the encounter frequency goes up, and for towing with stern seas (U is positive), the encounter frequency goes down. The encounter frequency was measured for a harmonic wave of frequency $\omega_0 = 1.0$ rad/sec at tow speeds from -6.0 m/s (towing into head seas) to 6.0 m/s (towing with stern seas). The resulting plot of ω_e vs. U is shown in Figure 3-1. The plot of ω_e vs. U is expected to be linear with a slope of $-\frac{\omega_0^2}{g}$ (see Eq. 3.3), which for $\omega_0 = 1.0$ rad/sec has a value of -0.1019 m^{-1}. The measured slope was -0.1017 m^{-1}, which shows the proper dependence of encounter frequency on speed has been captured.

Chapter 4

Exposure Statistics

The primary goal of the effort was to calculate exposure statistics as various design parameters were varied. However, before proceeding on to the exposure statistics results, the issue of "what constitutes an exposed (i.e., receiving) antenna element?" must be addressed. The experimentally observed performance characteristics of the "jelly roll" antenna elements drove this definition. It was found that for a level element in calm water the antenna gain is stable right up to the point at which the outer skin becomes completely submerged. It was also found that if any portion of the outer skin was covered by water (such as might happen in a wave field), then the gain of the element suffered drastically. Thus an exposed element was defined to be one which was exposed by some small threshold height (set to 0.04 *Diameter* for all simulations) at every point along the length of the element. In a discrete computer model some approximation is necessary with regard to "every point along the length of the element." Thus each antenna element was oversampled by an integer factor, M, which the user prescribes. Typical designs considered had an element length of 0.5 m, and were oversampled at $M = 8$.

4.1 Selection of Simulation Series

In order to bound the problem, it was necessary to discuss with the customer (U.S. Navy) what the operational profile required, and with designers (Lincoln Laboratory) what the engineering aspects of the antenna gain required. These discussions led to the following conclusions on the design space to be simulated:

- tow speed: $U \leq 10$ knots
- sea severity: $H_s \leq 3.0$ m (sea state 4 or less)
- length: vary about $L = 25$ m
- diameter: vary about $Diameter = 3$ inches
- density: vary about $\rho = 400$ kg/m^3
- antenna element length: vary about $L_{elem} = 0.5$ m.

In addition to performing simulation series to support the above design space, it was necessary to devote some simulations to verify that the results are, in fact, meaningful and consistent. Toward this end simulation series were made to

- compare exposure statistics results of the FFT and SWS methods
- vary duration of the simulation to determine what constitutes an adequate length of time.

It is not claimed that these simulation series represent an exhaustive list of all the parameters which could be varied, nor is it claimed that the model is completely verified by the consistency runs made. However the trends presented will be valuable for the design engineers as they consider performance trade-offs, and will allow them to better explore the design space of interest.

4.2 Results

4.2.1 Statistics Collected by the Model

The computer model was programmed to track three key statistics:

- average exposure – the average fraction of antenna elements exposed throughout the entire duration of the simulation
- threshold met – the average fraction of the time that some specified number of antenna elements (or more) were exposed

	x_1	x_2	x_3	x_4	x_5	x_N
t_0	0	1	1	0	1	1
t_1	1	0	1	1	0	0
t_2	1	1	0	0	1	1
t_3	0	1	1	0	1	1
t_4	1	0	1	1	1	0
t_T	0	1	1	0	0	1

Table 4.1: Exposure Data Matrix File Format

- average counterdetection length – the average length of the antenna completely exposed (i.e., completely out of the water).

(The counterdetection length, while not in the original list of desired statistics, was added because of the tactical significance of compromising submarine stealth.)

In addition, a record is made at each sample time of the condition of every antenna element, such that when the simulation is finished, an exposure matrix is available for further post-processing. The structure of the exposure matrix file (an ASCII text file) is shown in Table 4.1. (A "1" indicates an exposed antenna element, a "0" indicates a non-exposed element. The x_i represent antenna element locations, the t_i represent sample times.) Examples of information which could be extracted from the exposure matrix include

- average drop-out time of a specific element
- average (spatial) length of wave wash-overs
- histograms and standard deviations of the number of exposed elements
- exposure statistics for an array not fully populated (i.e., one could examine only the columns x_i which had antenna elements installed) .

Three output files are generated for each run of the computer model. They are the

- End-state summary file – lists input parameters used for the simulation, forces and velocities for the final time, and a summary of statistics collected

Parameter	Description
Method	SWS or FFT used to generate seas
H_s	significant wave height
Devel	sea development factor
$\omega_{\min}$	lowest wave frequency component
$\omega_{\max}$	highest wave frequency component
N_{freq}	number of (positive) wave frequency components
L	length of antenna
N_{elem}	number of antenna elements
L_{elem}	antenna element length
M	element oversample factor
Δs	antenna mesh size
Diameter	antenna diameter
ρ_{ant}	antenna density
EI	antenna stiffness
Duration	simulation duration
U	tow speed
N_{thresh}	threshold number of elements required for specified array gain

Table 4.2: Simulation Parameter List

- Exposure data matrix file – provides exposure condition of each element at each specified time increment (refer to Table 4.1)
- Snapshot file – provides a visual display of the antenna as it floats on the sea surface.

These output files are described in greater detail in Appendix A.

The input parameters which are specified for each run of the computer model are listed in Table 4.2.

In the exposure statistics results given below, each series of simulations is presented in the following manner:

- the parameter input table used in the series is listed
- plots are provided of the three exposure statistics tracked
  - average fraction of elements exposed
  - fraction of the time that the threshold number of elements were exposed
  - average counterdetectable length of the antenna

It is important to realize that these plots represent averages in time and space. This is necessary in order to display the results as functions of key antenna design parameters (length, diameter, etc.), which is most useful from a designer's viewpoint. From the output files, it is also possible to analyze how the statistics vary as time progresses, or how the statistics vary down the array from the tow point to the trailing end. Because of the large number of simulation runs, only a few representative plots of this type of information will be shown.

Parameter	Description
Method	SWS
H_s	various
Devel	1.0
$\omega_{\min}$	0.4 rad/sec
$\omega_{\max}$	24.0 rad/sec
N_{freq}	700
L	25 m
N_{elem}	50
L_{elem}	0.5 m
M	8
Δs	0.0625 m
Diameter	3.0 inch
ρ_{ant}	408 kg/m^3
EI	0 Pa m^4
Duration	180 sec
U	various
N_{thresh}	40

Table 4.3: Series 1 Input Parameters

4.2.2 Series 1: Statistics vs. Sea Severity and Tow Speed

Input

The input parameters for Series 1: Statistics vs. Sea Severity and Tow Speed, are given in Table 4.3. The tow speeds used were 3, 5, 7, and 9 knots; the significant wave heights used were 0.5, 1.0, 1.5, 2.0, 2.5, and 3.0 meters.

Results

Average fraction of elements exposed. Figure 4-1 shows a rather weak dependence of the average fraction of elements exposed versus significant wave height, decreasing as the sea severity increases. However, the plot shows a strong dependence of average exposure versus tow speed.

Fraction of time threshold met. With a required threshold of 40 out of 50 elements, Figure 4-2 again shows that tow speed is the dominant factor in the exposure probabilities.. The slight rise in threshold met versus significant wave height for the 7 and 9 knot data is an interesting feature, which will be discussed further below.

Average counterdetection length. As one would expect, Figure 4-3 shows the average length of the antenna totally exposed increases with tow speed and sea state. The tow speed contributes added tension in the antenna, and the wave height provides the troughs necessary for a section to become exposed.

Histogram Analysis for Number of Exposed Elements

As mentioned above, there is slight rise in 'threshold met' for 7 and 9 knot runs as the sea severity increases. This is not obvious at first, but can be explained as follows. Figures 4-4 - 4-6 show the histograms of the number of exposed elements over time running at 7 knots in significant wave heights of 1.0, 2.0, and 3.0 meters. For low sea states, the waves have little energy, and thus have little ability to affect the exposure statistics. This leads to a relatively tightly grouped distribution, as in Figure 4-4. Because the mean is below the threshold required, the 'threshold met' is very low. (As in Figure 4-2.) But as the significant wave height increases, the waves contain more energy, and cause greater variation in the exposure statistics. This causes the distributions to flatten out, while the mean exposure stays relatively constant. As the upper tail of the distribution moves outward from the mean, it provides more "hits" above the required threshold of 40 elements. This trend is confirmed in Figures 4-5 and 4-6.

4.2.3 Series 2: Statistics vs. Length

Input

The input parameters for Series 2: Statistics vs. Length, are given in Table 4.4. The threshold number of elements was varied in proportion to the length (and the number of elements), but was kept at 80% of the total number of elements. Element length was kept constant.

Results

Average fraction of elements exposed. The average fraction of elements exposed drops off quickly at first, then becomes nearly flat, as shown in Figure 4-7. This effect must be studied more closely, since the boundary conditions have a much greater relative impact on a short antenna than a long one. (Recall the tow point and trailing end are set to float at the sea surface.)

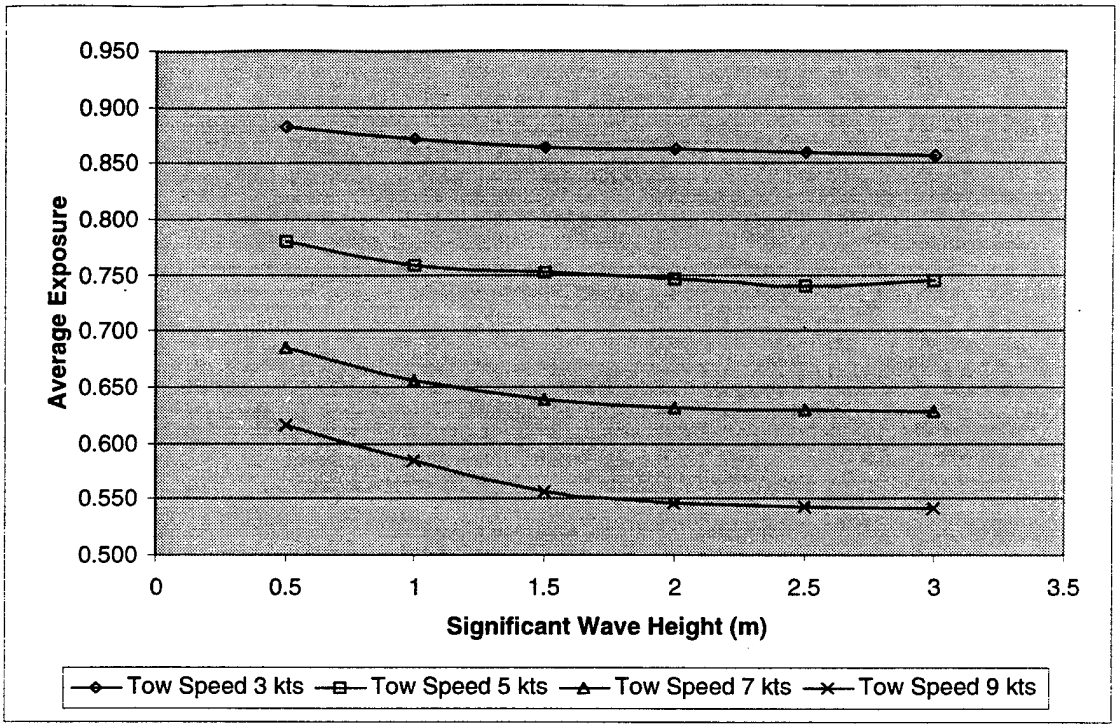

Figure 4-1: Average Exposure vs. Tow Speed and Significant Wave Height

Parameter	Description
Method	SWS
H_s	2.5 m
Devel	1.0
$\omega_{\min}$	0.4 rad/sec
$\omega_{\max}$	24.0 rad/sec
N_{freq}	700
L	various
N_{elem}	various
L_{elem}	0.61 m
M	10
Δs	0.061 m
Diameter	3.0 inch
ρ_{ant}	408 kg/m^3
EI	0 Pa m^4
Duration	180 sec
U	5 knots
N_{thresh}	various ($0.8\,N_{elem}$)

Table 4.4: Series 2 Input Parameters

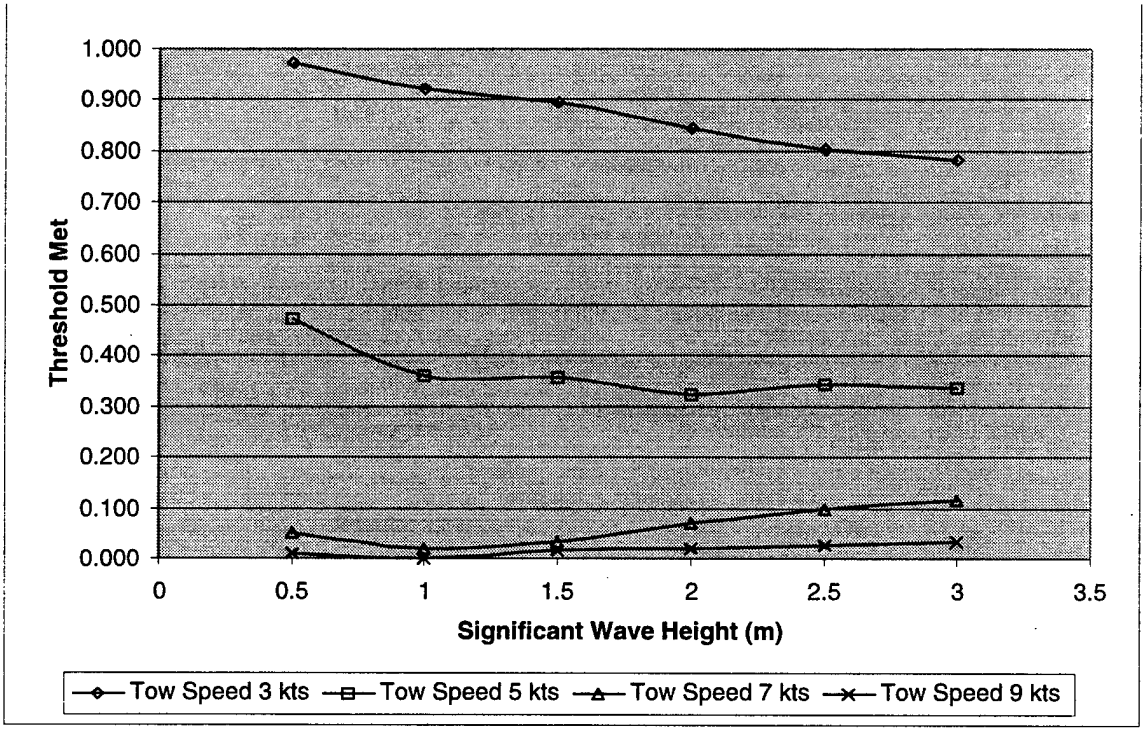

Figure 4-2: Threshold Met vs. Tow Speed and Significant Wave Height

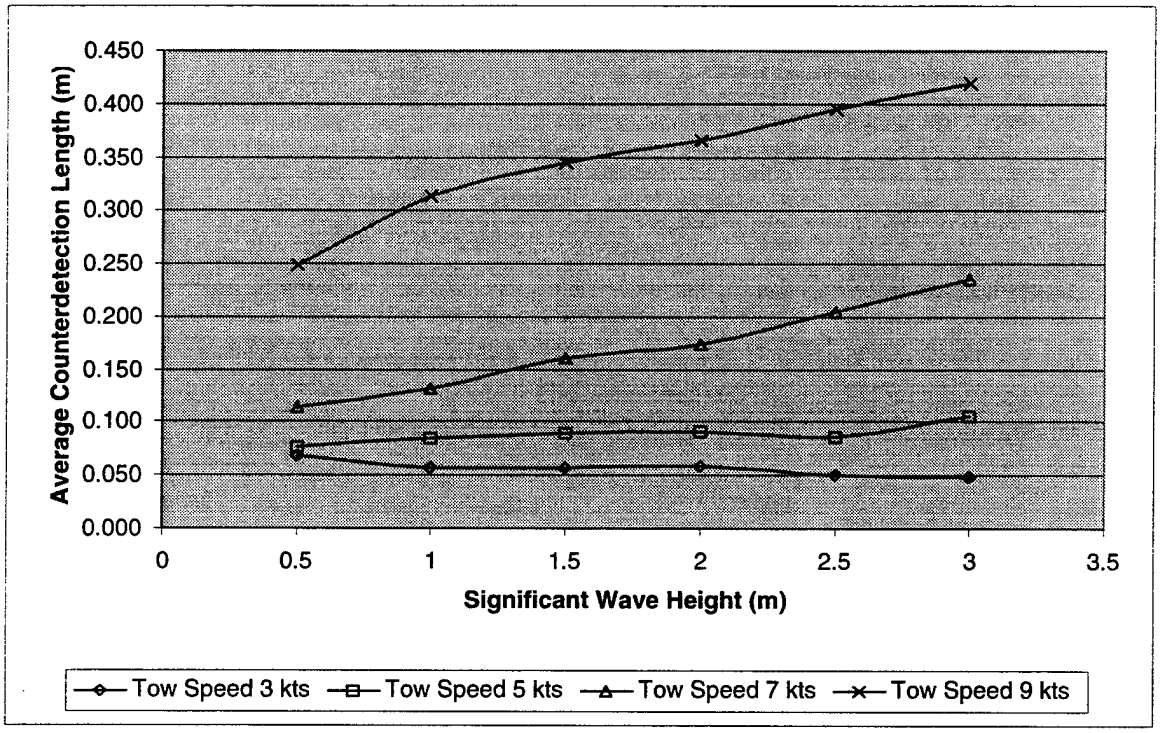

Figure 4-3: Counterdetection Length vs. Tow Speed and Significant Wave Height

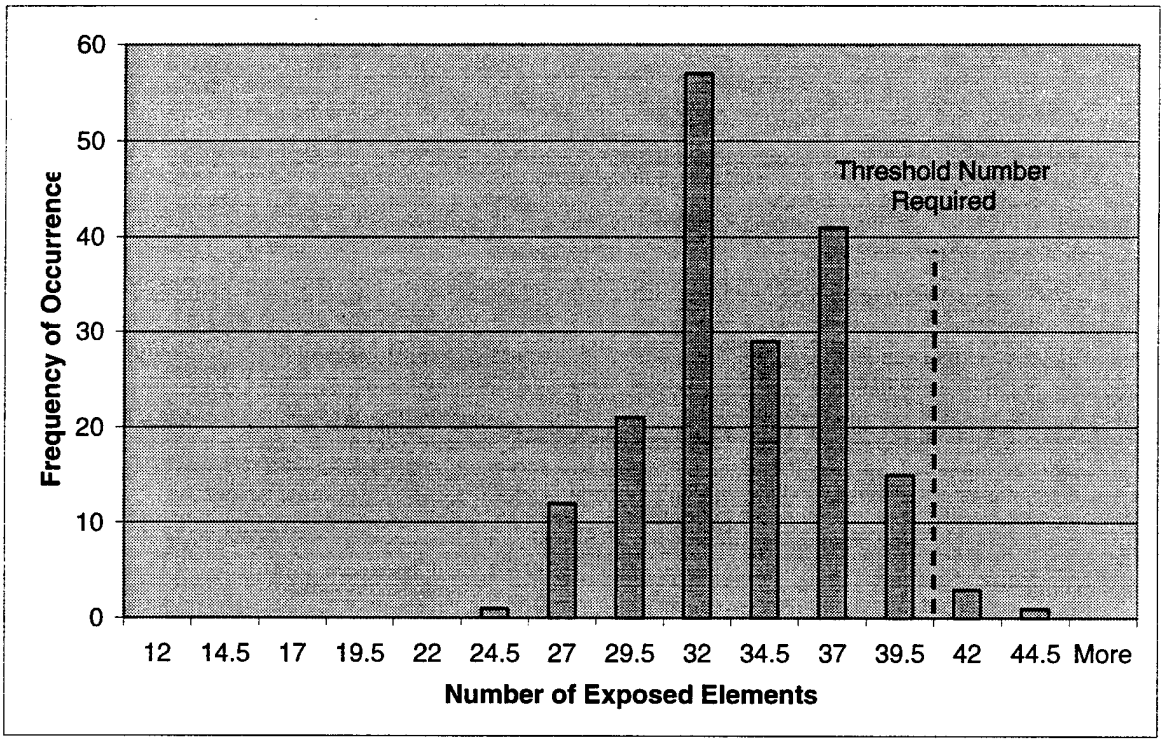

Figure 4-4: Histogram of Exposed Number of Elements at 7 kts: H_s= 1.0 m

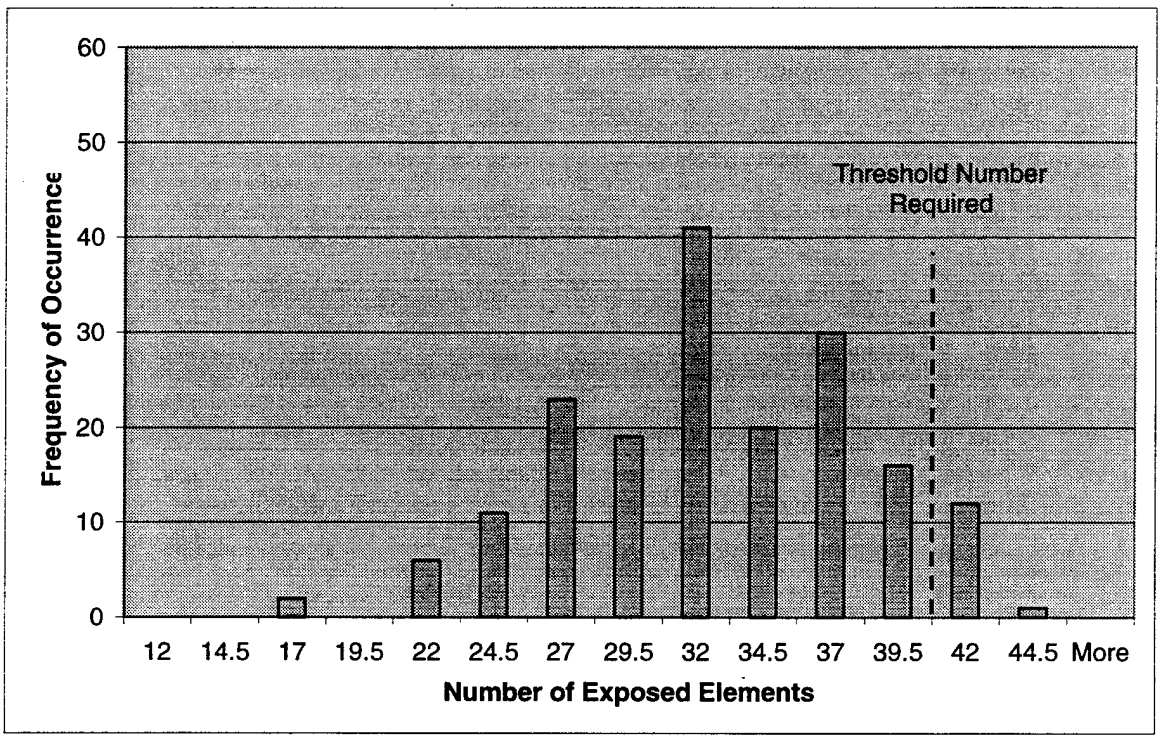

Figure 4-5: Histogram of Exposed Number of Elements at 7 kts: $H_s = 2.0$ m

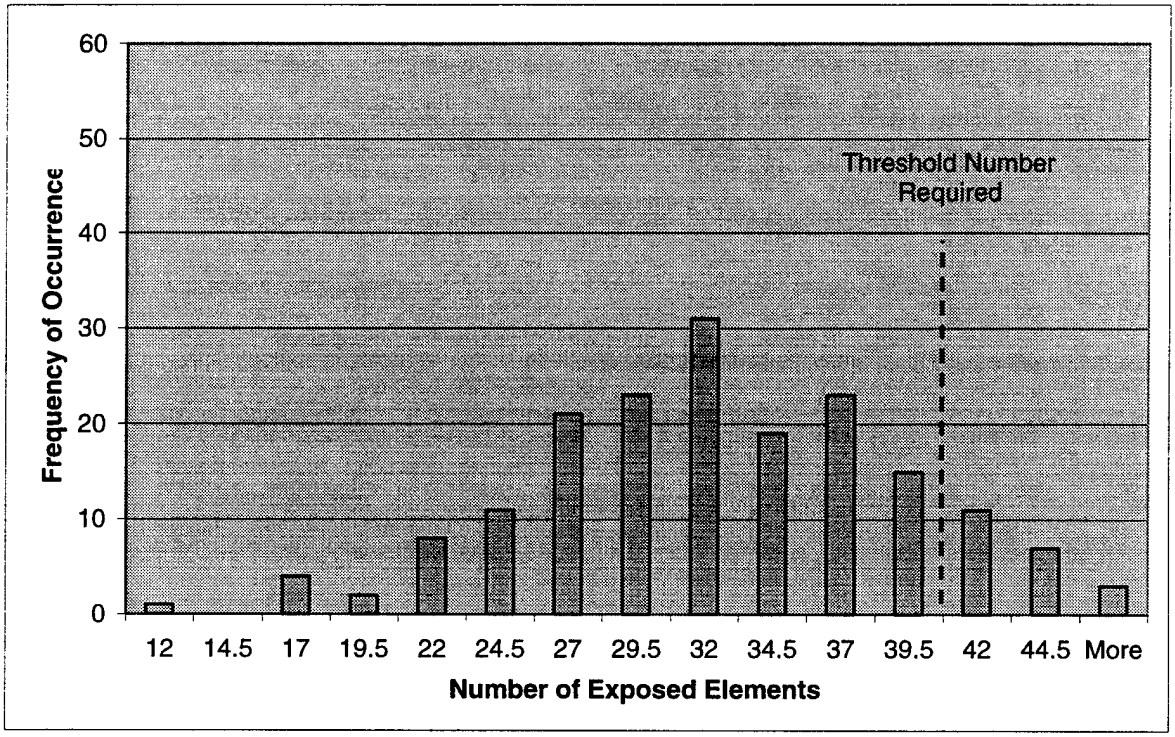

Figure 4-6: Histogram of Number of Exposed Elements at 7 kts: H_s= 3.0 m

Parameter	Description
Method	FFT
H_s	2.5 m
Devel	1.0
$\omega_{\min}$	0.347 rad/sec
$\omega_{\max}$	22.206 rad/sec
N_{freq}	4096
L	25 m
N_{elem}	various
L_{elem}	various
M	various
Δs	0.0625 m
Diameter	3.0 inch
ρ_{ant}	408 kg/m^3
EI	0 Pa m^4
Duration	180 sec
U	5 knots
N_{thresh}	various ($0.8\,N_{elem}$)

Table 4.5: Series 3 Input Parameters

Fraction of time threshold met. Because the threshold was kept at 80% of the total number of elements, we see a sharp drop off in the threshold met versus length in Figure 4-8. If the threshold were maintained at some constant number of elements (e.g., 15), one would see the opposite trend as length increased.

Average counterdetection length. The rise in counterdetection length in Figure 4-9 is a combination of two factors: maximum tension grows proportional to the length, and as antenna length grows beyond the average wavelength it bridges the wave peaks more often.

4.2.4 Series 3: Statistics vs. Element Length

Input

The input parameters for Series 3: Statistics vs. Element Length, are given in Table 4.5. The total antenna length was held at 25 meters, and the element lengths used were 0.25, 0.5, 1.0, and 5.0 meters. The oversample factor M was varied to keep the antenna mesh length Δs constant at 0.0625 meters.

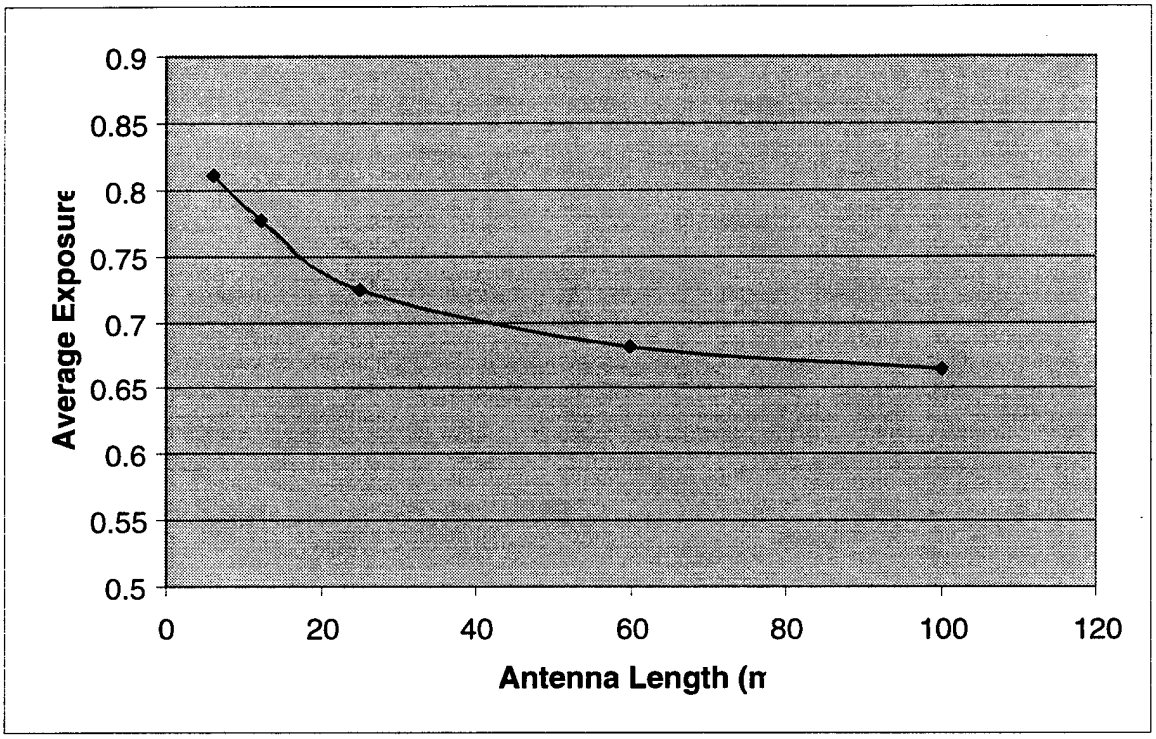

Figure 4-7: Average Exposure vs. Length

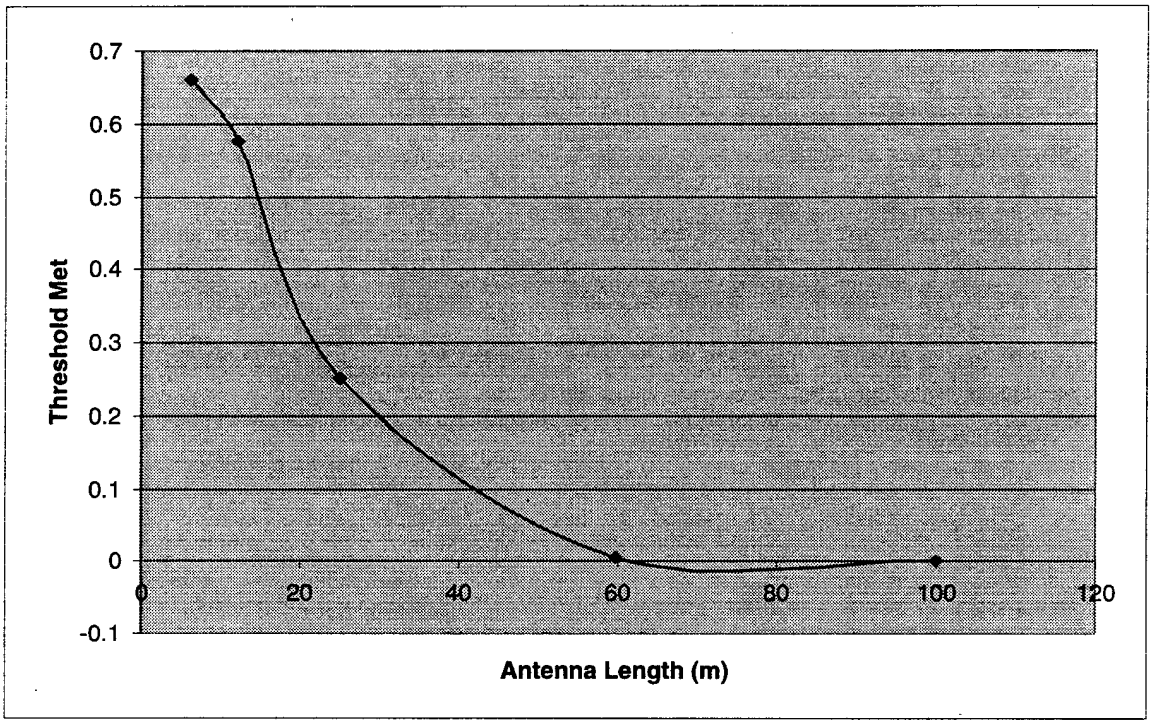

Figure 4-8: Threshold Met vs. Length

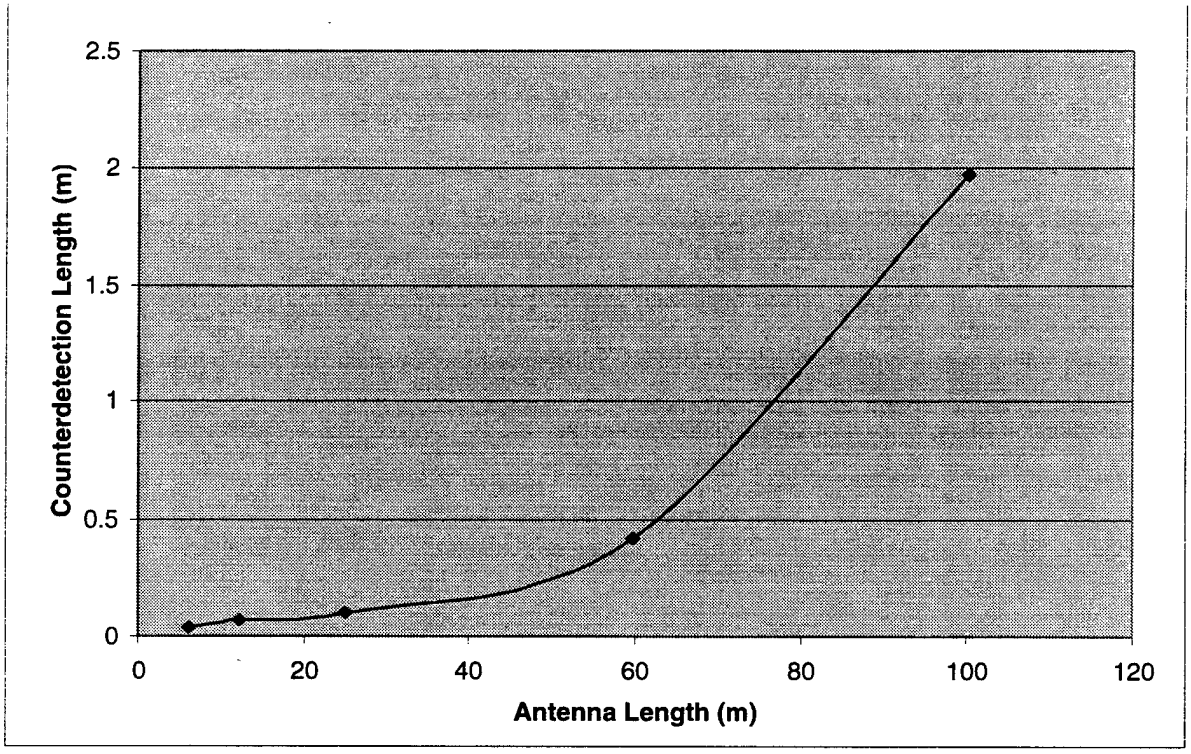

Figure 4-9: Counterdetection Length vs. Length

Results

Average fraction of elements exposed. The results in Figure 4-10 show the effect of requiring that a contiguous length (the element length) be exposed. As the contiguously exposed length requirement grows, the probability of meeting it decreases.

Fraction of time threshold met. Figure 4-11 shows that the threshold met drops drastically as element length grows. The reason can be traced back to Figure 4-10, which shows the mean exposure falls below the threshold of 80%. The more the average exposure falls below the required threshold number of elements, the more rapidly the 'threshold met' drops off toward zero. This pattern would be expected for any distribution with central tendencies. ("Central tendency" distributions are distributions which have a higher probability of returning a value near the mean than values far away from the mean. The normal (bell-shaped) distribution is a classic example of a distribution with a central tendency.)

Average counterdetection length. Varying the element length should have no effect on the totally exposed length (the elements are assumed to have flexibility given by EI). Figure 4-12 supports this claim.

4.2.5 Series 4: Statistics vs. Diameter

Input

The input parameters for Series 4: Statistics vs. Diameter, are given in Table 4.6. All parameters were held constant, except for the antenna outer diameter, which took on values of 1.0, 2.0, 3.0, and 5.0 inches.

Results

Average fraction of elements exposed. The average fraction of elements exposed is a strong function of antenna diameter, as seen in Figure 4-13. This is to be expected, since antenna tension and normal drag forces (per unit length) grow proportional to the diameter, and buoyancy forces (per unit length) grow as diameter squared.

Fraction of time threshold met. (Figure ??) Typical for distributions with central tendencies, and a mean which varies as in Figure 4-13.

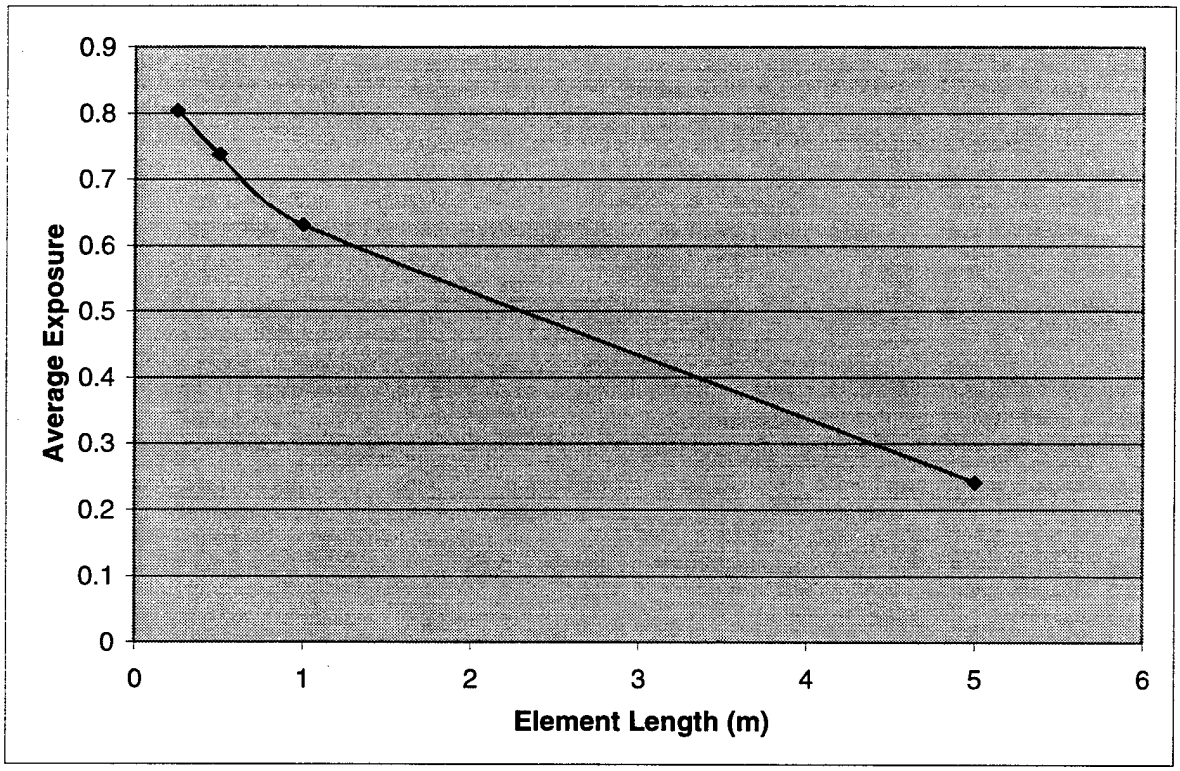

Figure 4-10: Average Exposure vs. Element Length

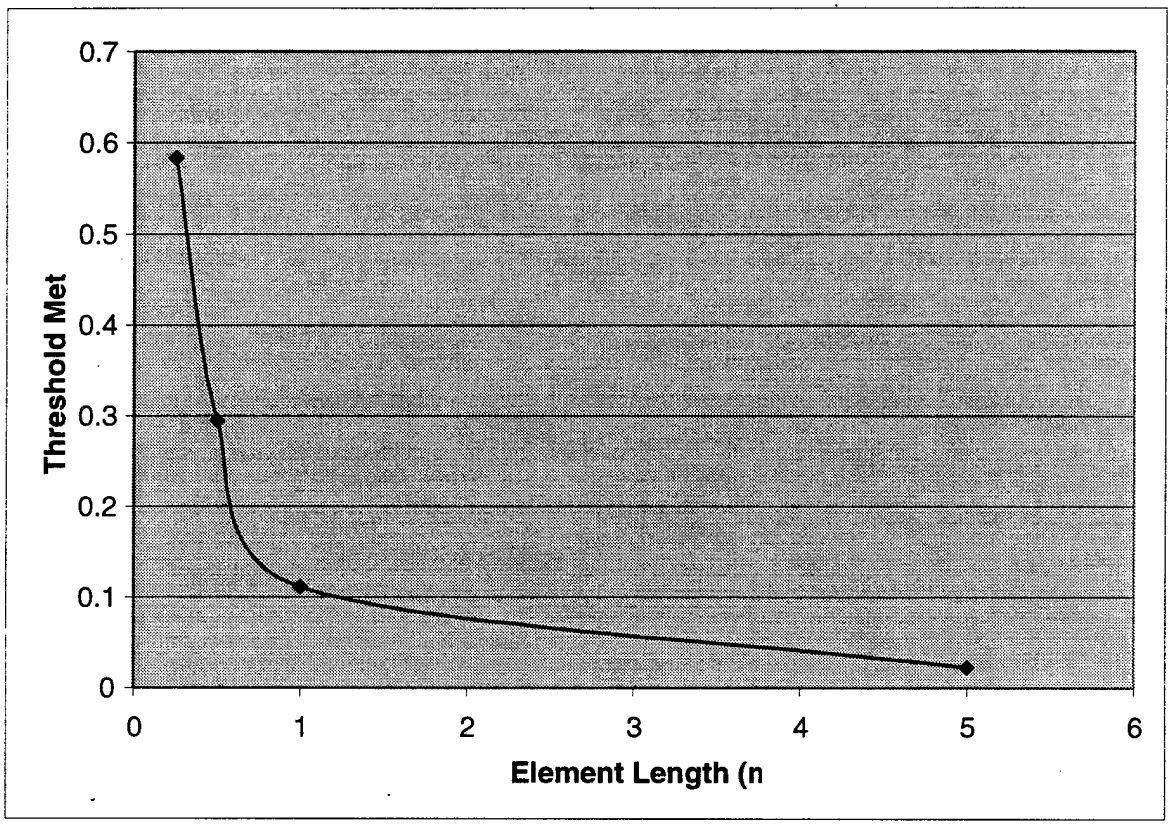

Figure 4-11: Threshold Met vs. Element Length

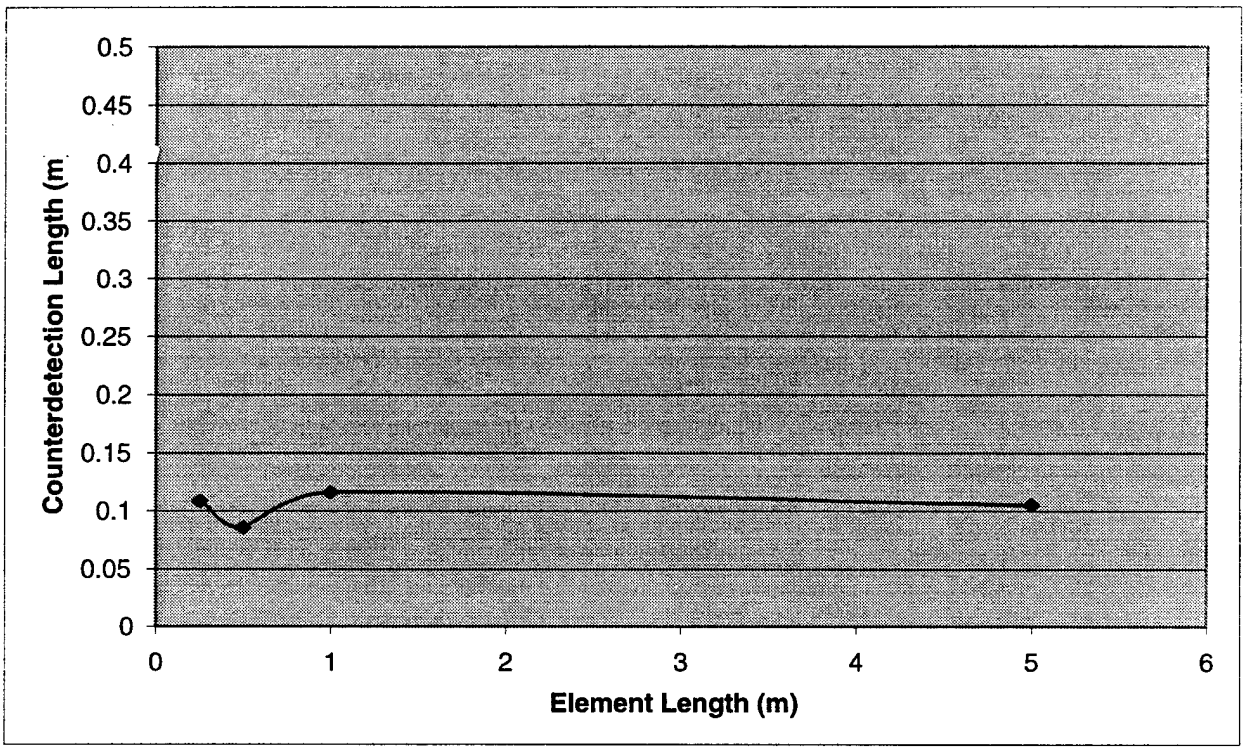

Figure 4-12: Counterdetection Length vs. Element Length

Parameter	Description
Method	FFT
H_s	2.5 m
Devel	1.0
$\omega_{\min}$	0.347 rad/sec
$\omega_{\max}$	22.206 rad/sec
N_{freq}	4096
L	25 m
N_{elem}	50
L_{elem}	0.5 m
M	8
Δs	0.0625 m
Diameter	various
ρ_{ant}	408 kg/m^3
EI	0 Pa m^4
Duration	180 sec
U	5 knots
N_{thresh}	40

Table 4.6: Series 4 Input Parameters

Average counterdetection length. Figure 4-15 shows a strong dependence of counterdetection length on diameter. This is again because the buoyancy forces depend on diameter squared, and thus large diameter designs "ride" the waves, instead of cutting through them.

4.2.6 Series 5: Statistics vs. Density

Input

The input parameters for Series 5: Statistics vs. Density, are given in Table 4.7. All parameters were held constant, except for the antenna density, which took on values of 200, 300, 408, 500, 600, and 700 kg/m^3. (The density of the prototype antenna element is 408 kg/m^3.)

Results

Average fraction of elements exposed. The result shown in Figure 4-16 looks very much like an inverse of the result from the previous series. This is because the downward weight force (per unit length) grows proportional to the density, while other forces modeled remain unaffected as the antenna density varies.

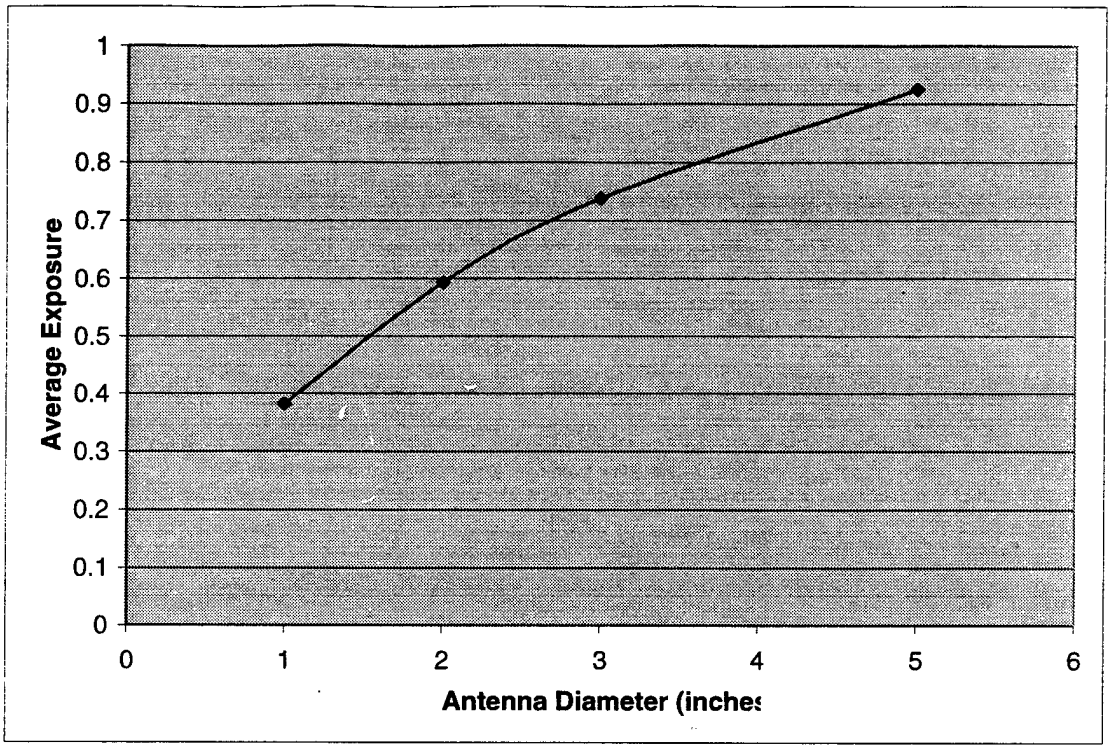

Figure 4-13: Average Exposure vs. Diameter

Parameter	Description
Method	FFT
H_s	2.5 m
Devel	1.0
$\omega_{\min}$	0.347 rad/sec
$\omega_{\max}$	22.206 rad/sec
N_{freq}	4096
L	25 m
N_{elem}	50
L_{elem}	0.5 m
M	8
Δs	0.0625 m
Diameter	3.0 inch
ρ_{ant}	various
EI	0 Pa m^4
Duration	180 sec
U	5 knots
N_{thresh}	40

Table 4.7: Series 5 Input Parameters

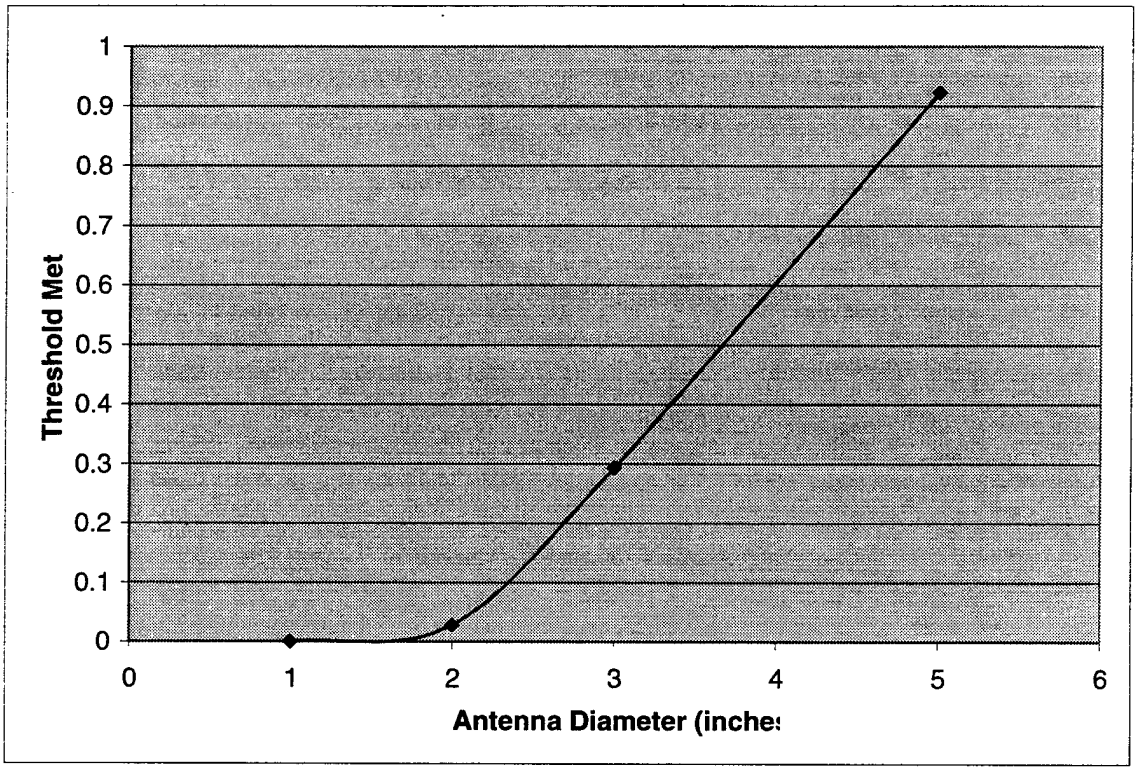
Threshold Met
1
0.9
0.8
0.7
0.6
0.5
0.4
0.3
0.2
0.1
0
0
1
2
3
4
5
6
Antenna Diameter (inches

Figure 4-14:

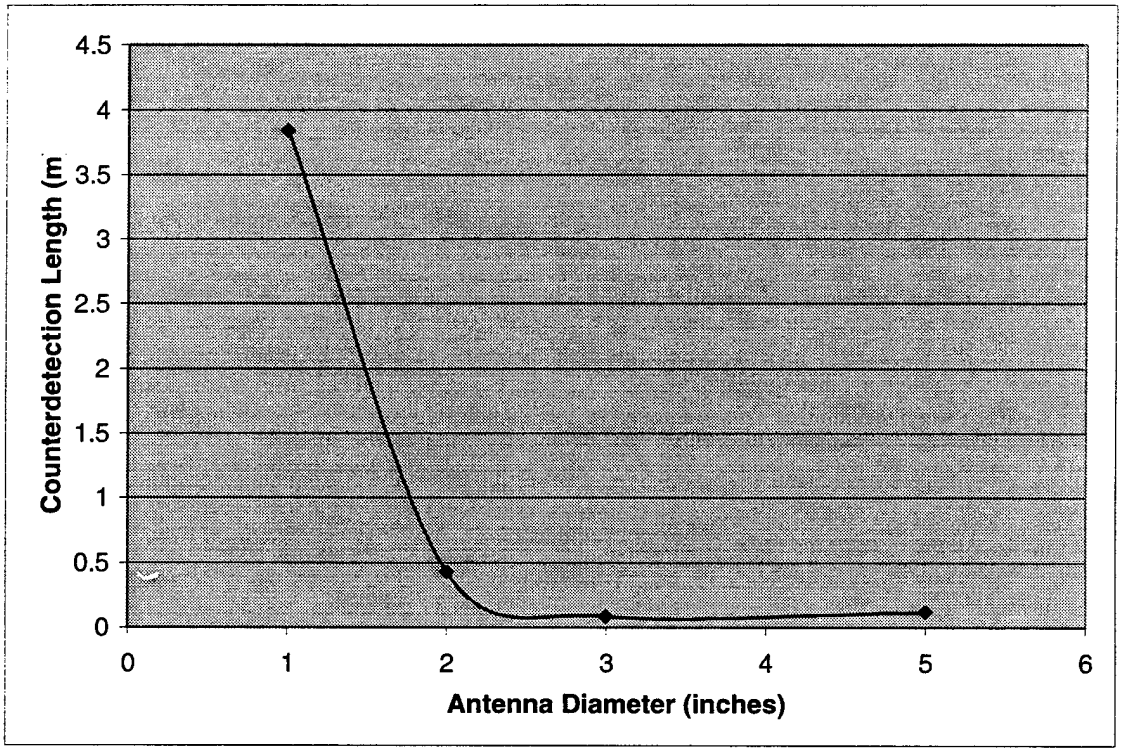

Figure 4-15: Counterdetection Length vs. Diameter

Fraction of time threshold met. (Figure 4-17) Typical for distributions with central tendencies, and a mean which varies as in Figure 4-16.

Average counterdetection length. Figure 4-18 shows a knee in the curve at the 408 kg/m^3 density. While other factors shift this knee left or right, the density of the prototype antenna element happens to be about the lowest value one would desire from a counterdetection standpoint at this speed-sea state combination. So from a connectivity viewpoint, lower density is desirable; from a stealth viewpoint, lower density is not desirable. Such trade-offs occur routinely in submarine operations.

4.2.7 Series 6: Statistics vs. Duration

This series and the one following are intended to support the credibility of the above simulation results. The purpose of this validation series was to demonstrate that the 180 second duration used in the computer runs was long enough to be representative of a random process. There were two conflicting goals with regard to the duration:

- computer run time dictated the shortest duration feasible
- statistical confidence dictated the longest duration possible.

Thus three runs were conducted at three different durations (for a total of nine runs), in order to understand the variance involved in the statistics presented in the first 5 series of simulations.

Input

The input parameters for Series 6: Statistics vs. Duration, are given in Table 4.8. Three runs each were made for duration values of 60, 180, and 720 seconds.

Results

Referring to Figures 4-19 - 4-21, each duration has three bars plotted which correspond to the three runs made for that duration. The dashed lines represent the best estimate of the actual statistic plotted, since it is the average of the three 720 second run results. Above each duration

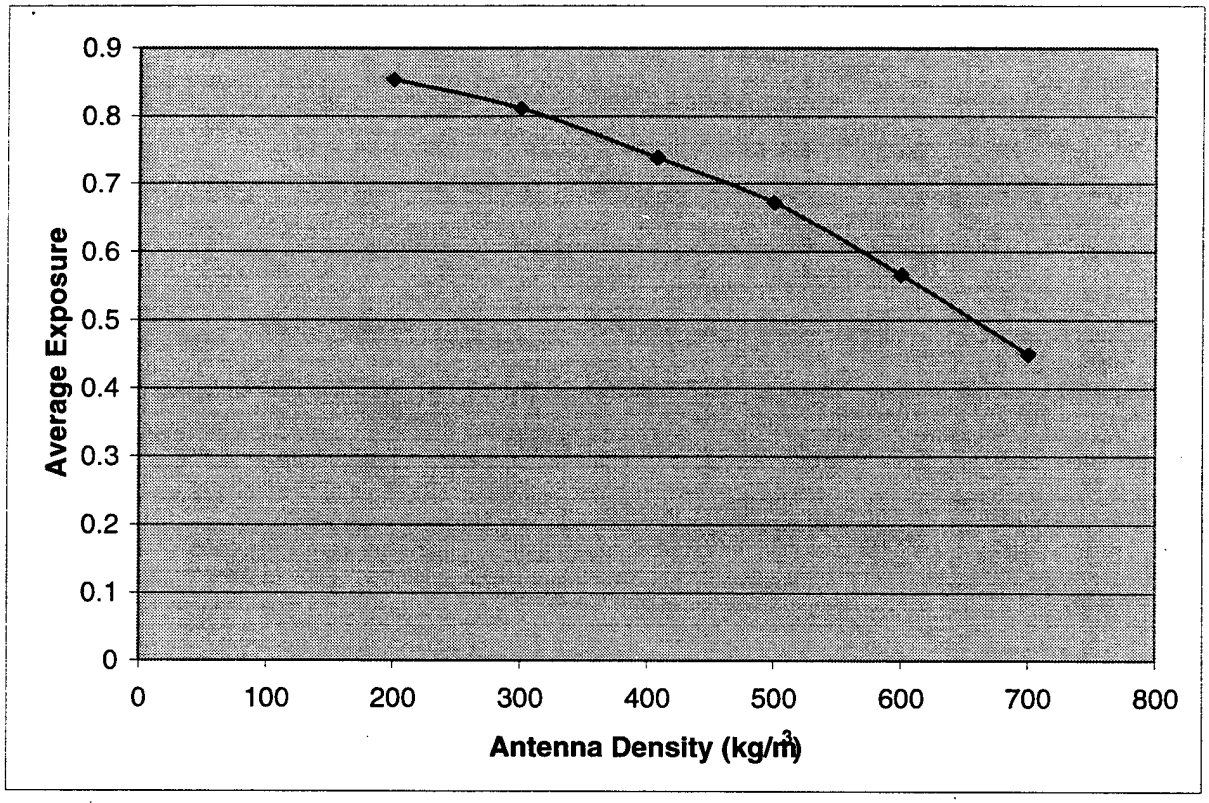

Figure 4-16: Average Exposure vs. Density

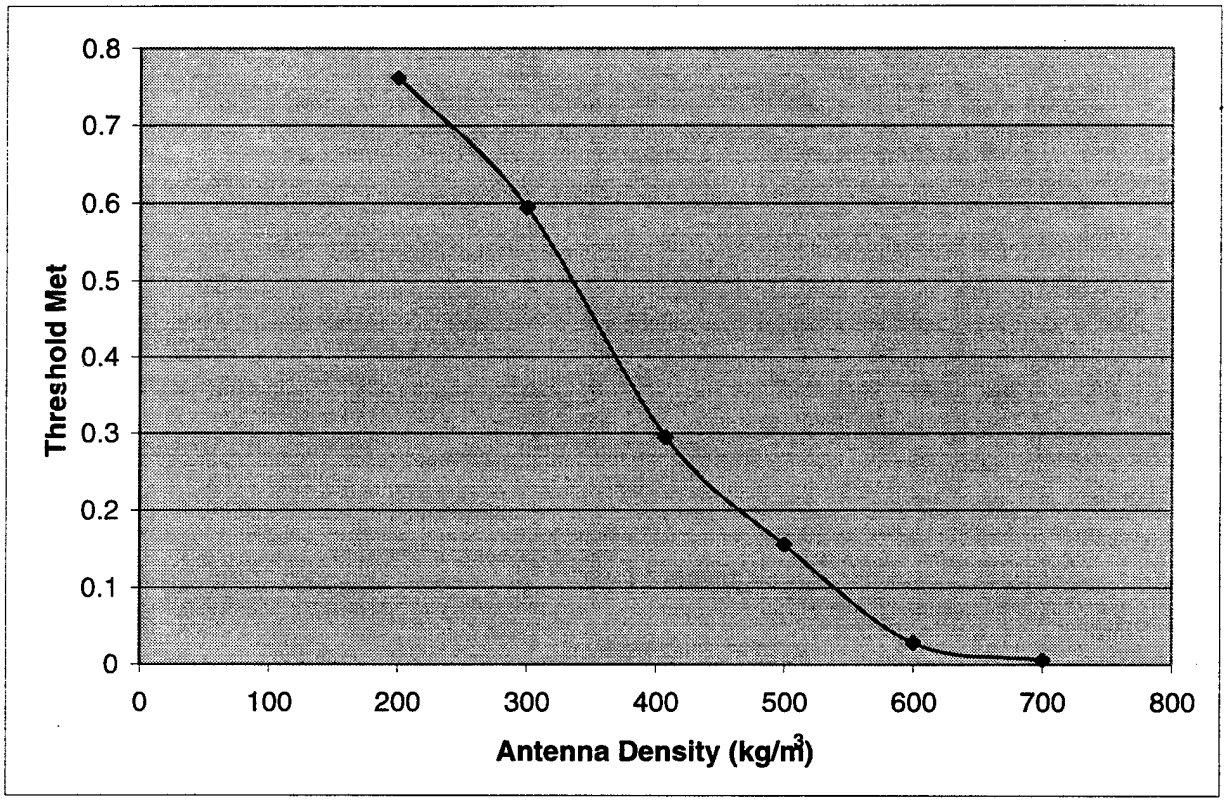

Figure 4-17: Threshold Met vs. Density

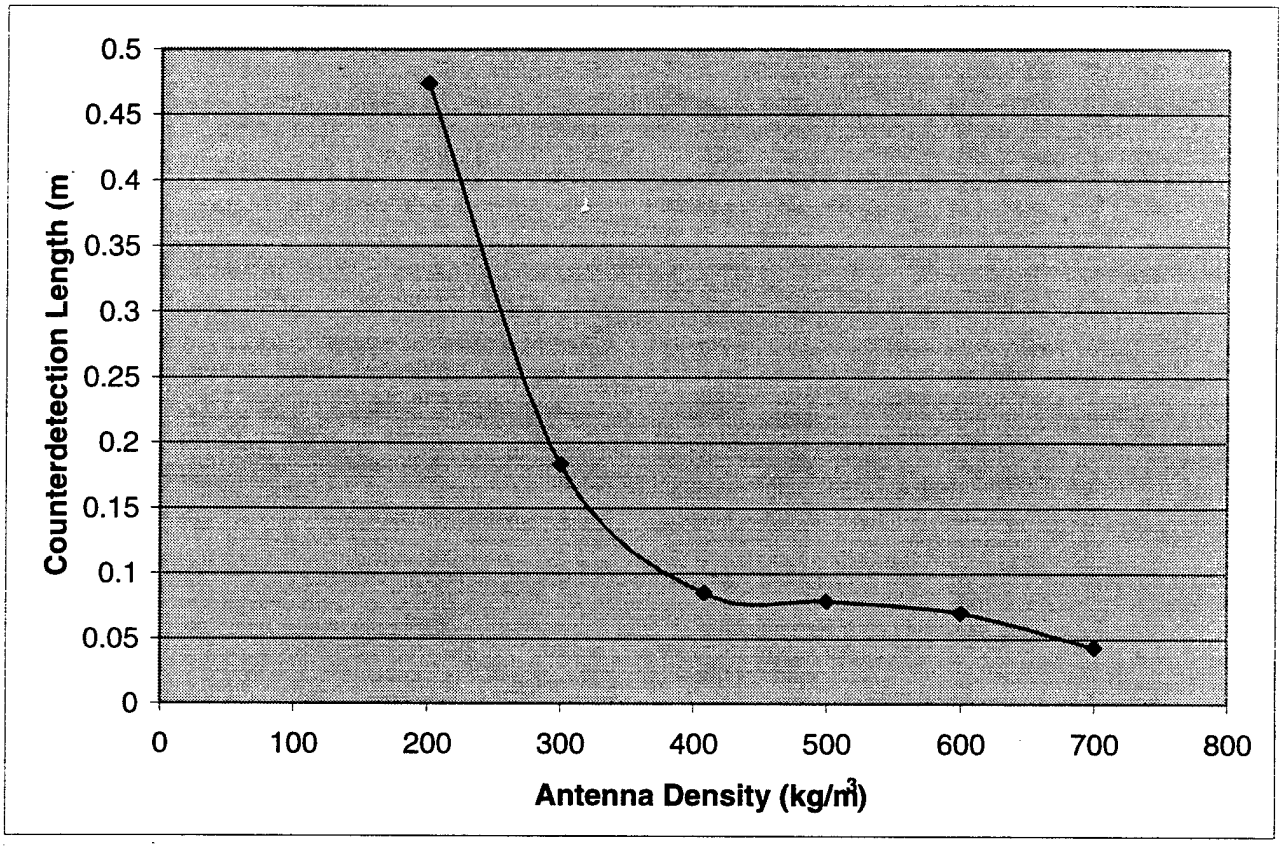

Figure 4-18: Counterdetection Length vs. Density

Parameter	Description
Method	FFT
H_s	2.5 m
Devel	1.0
$\omega_{\min}$	0.347 rad/sec
$\omega_{\max}$	22.206 rad/sec
N_{freq}	4096
L	25 m
N_{elem}	50
L_{elem}	0.5 m
M	8
Δs	0.0625 m
Diameter	3.0 inch
ρ_{ant}	408 kg/m^3
EI	0 Pa m^4
Duration	various
U	5 knots
N_{thresh}	40

Table 4.8: Series 6 Input Parameters

value is the mean and standard deviation associated with those three simulations. As expected, the longer the simulation lasts, the smaller the standard deviation becomes. The goal of the computer model is to show trends which will assist the designers in choosing the optimum antenna parameters. At this stage of the simulation effort, the precise values for element exposure cannot be predicted without more extensive experimental validation efforts. Thus the standard deviation associated with the 180 second duration was judged to be a satisfactory compromise between computer run time and statistical confidence.

4.2.8 Series 7: Statistics vs. Sea Generation Method

Input

This series ran identical parameters (within the limits of the meshing conditions) using the SWS and the FFT method, in order to ensure the results were consistent between the methods. Table 4.9 shows the values used, and indicates which parameters were not matched exactly because of frequency meshing issues. The significant wave height was set to 1.0 and 3.0 meters, in order to compare the methods over the full range of sea states simulated.

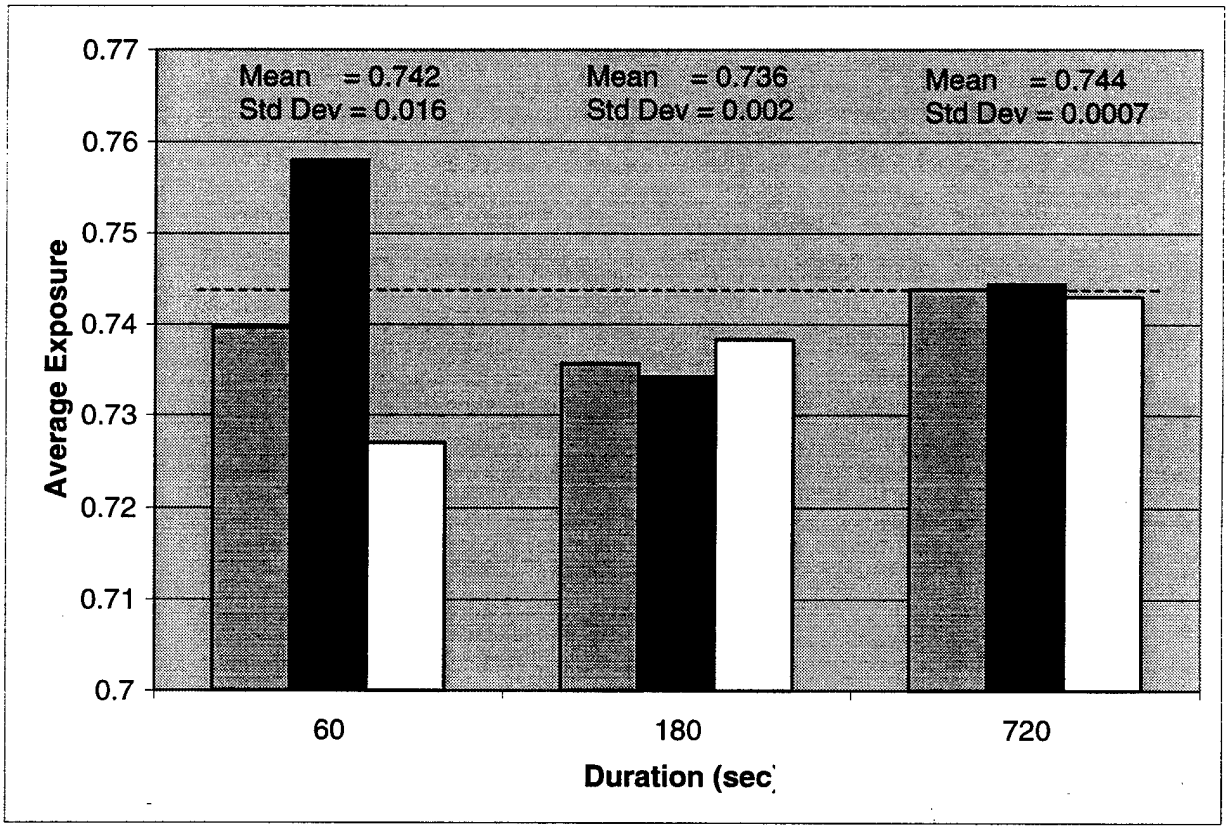

Figure 4-19: Average Exposure vs. Duration

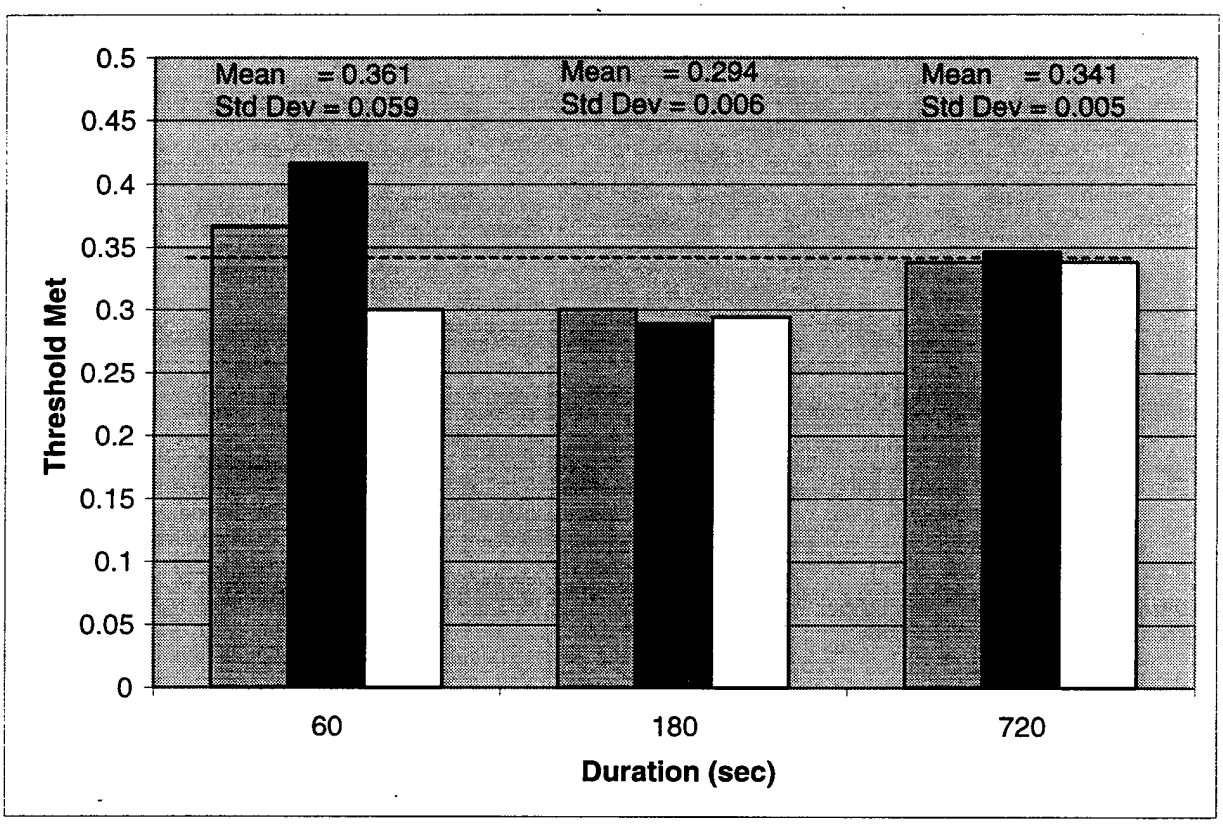

Figure 4-20: Threshold Met vs. Duration

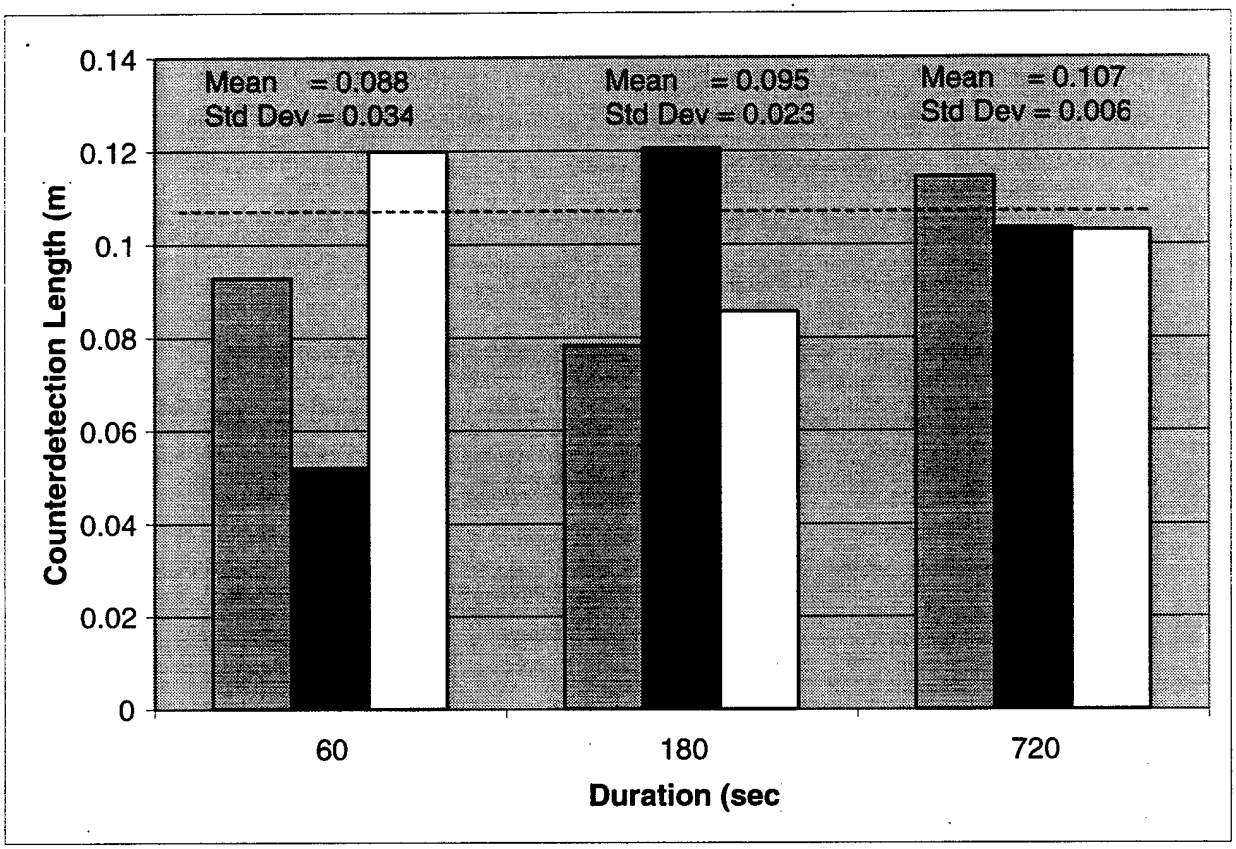

Figure 4-21: Counterdetection Length vs. Duration

Parameter	Description
Method	FFT / SWS
H_s	Various
Devel	1.0
$\omega_{\min}$	0.347 / 0.4 rad/sec
$\omega_{\max}$	22.206 / 24.0 rad/sec
N_{freq}	4096 / 700
L	25 m
N_{elem}	50
L_{elem}	0.5 m
M	8
Δs	0.0625 m
Diameter	3.0 inch
ρ_{ant}	408 kg/m^3
EI	0 Pa m^4
Duration	180 sec
U	Various
N_{thresh}	40

Table 4.9: Series 7 Input Parameters

Results

Figures 4-22 - 4-25 compare the results between the FFT and SWS methods. The agreement between the methods is very good; the differences are on the order of the standard deviations found in the previous section.

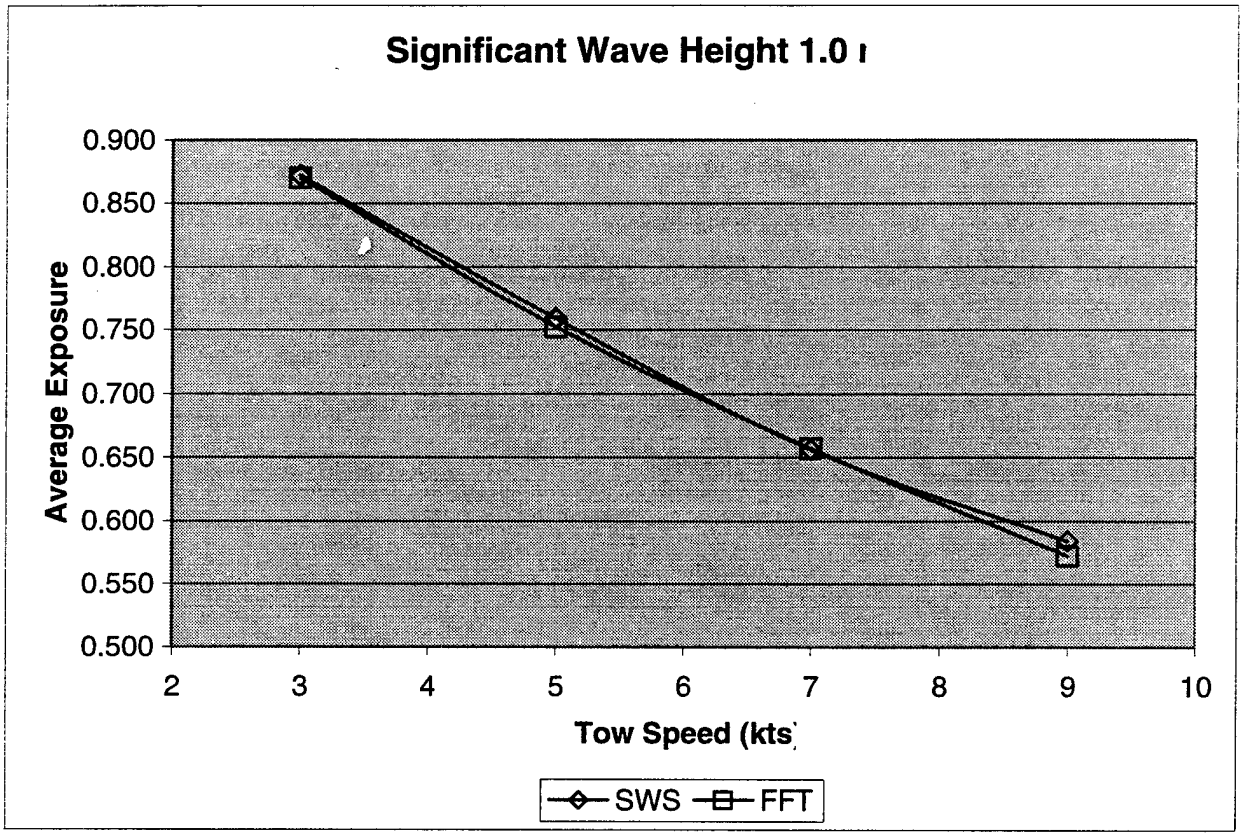

Figure 4-22: Comparison of SWS and FFT Methods: Average Exposure for 1.0 m H_s

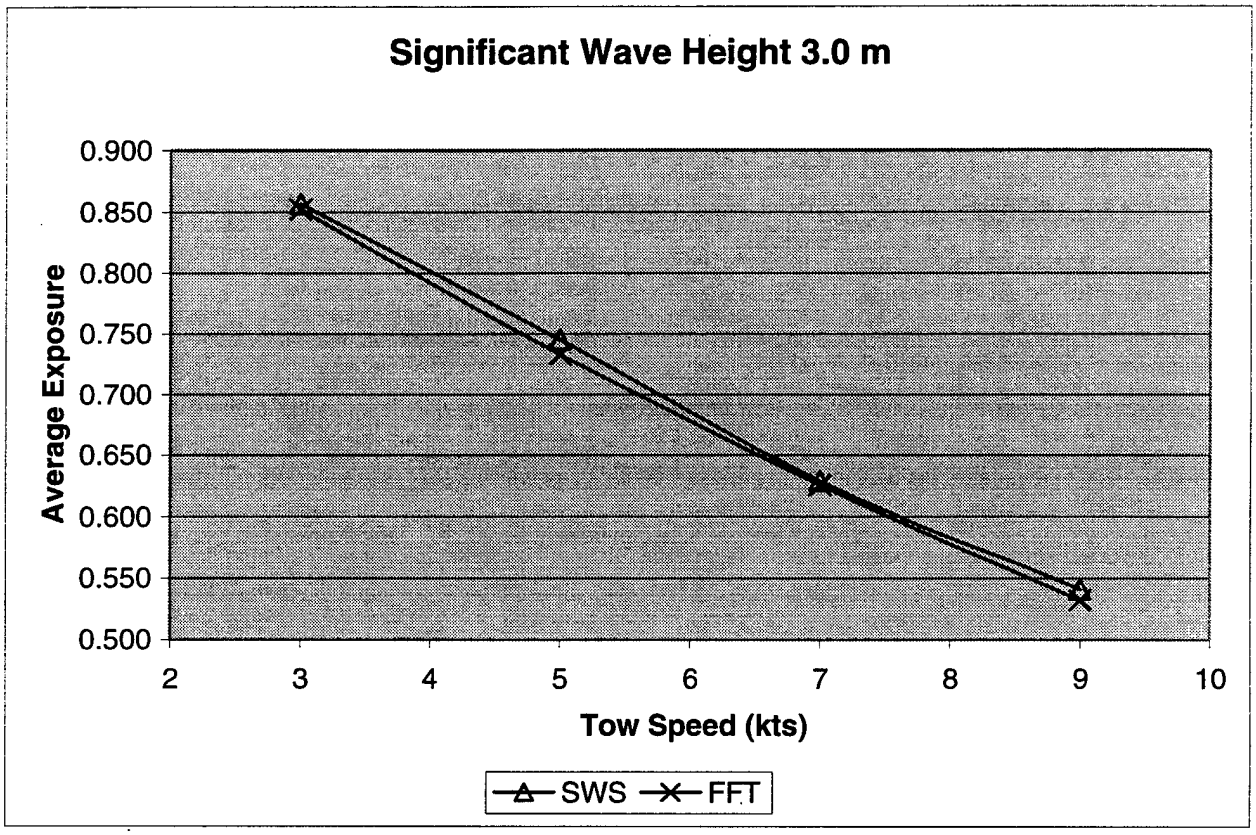

Figure 4-23: Comparison of SWS and FFT Methods: Average Exposure for 3.0 H_s

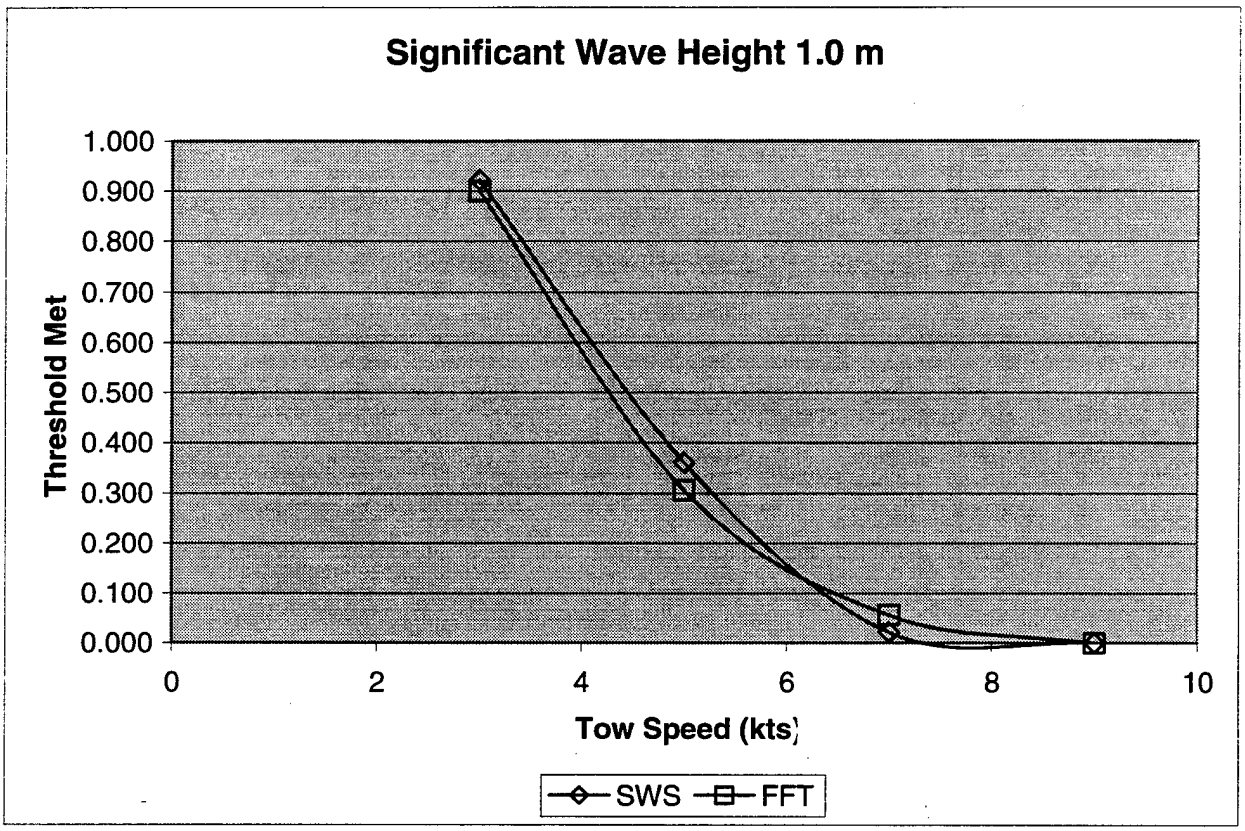

Figure 4-24: Comparison of SWS and FFT Methods: Threshold Met for 1.0 m H_s

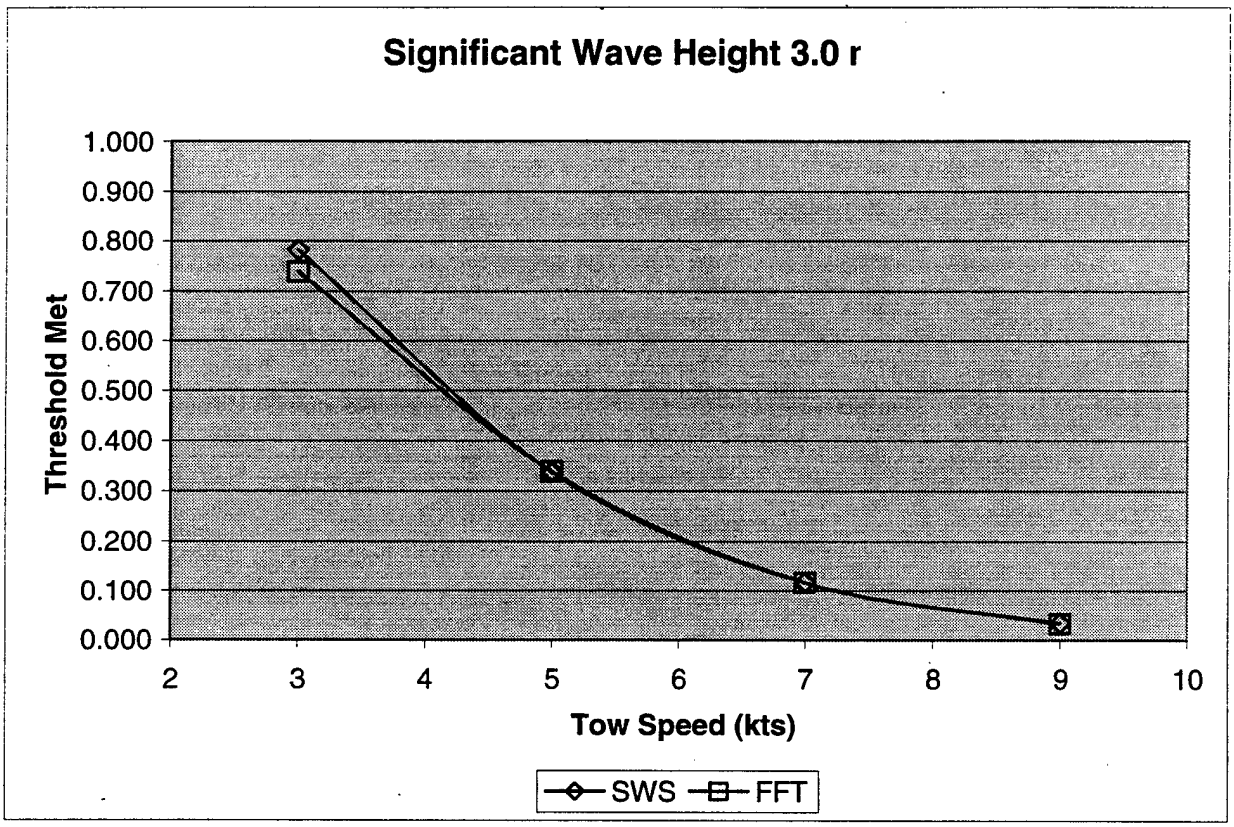

Figure 4-25: Comparison of SWS and FFT Methods: Threshold Met for 3.0 m H_s

Chapter 5

Future Efforts

The Buoyant Cable Array Antenna ATD is funded for FY 99 and FY 00. Should this proof-of-concept phase show that the floating antenna principles are feasible and cost effective, the Navy is expected to fund the development of a design which can stand up to the rigors of fleet deployment. Lincoln Laboratory is scheduled to test a prototype antenna in June 1999 off the coast of Hawaii. Data will be collected on the electromagnetic performance of the antenna elements under varying conditions of source strength, source elevation angle, and source azimuthal angle. In addition, the testing will document sea state and towing speeds so that performance can be related to the sea environment.

Work at MIT will continue to support the floating antenna effort. Another graduate student, under the supervision of Professor Jerome Milgram, will continue and extend the scope of the simulation effort. Areas which will be investigated to improve the capability of the computer model include

- 2 dimensional modeling of the sea surface
- arbitrary angle between tow heading and direction of seas
- more detailed modeling of the hydrodynamics at the free surface
- higher order integration schemes
- validation against at-sea test data.

Appendix A

User's Guide to *Antenna*

The User's Guide is broken down into two sections:

- Input File
- Output File.

Section A.1 will go through the *Antenna_FFT* input file line by line, and include program features or limitations associated with each parameter. At the end, features unique to the *Antenna_SWS* input file will be addressed. Section A.3 will briefly describe the contents of each of the three output files, and recommended methods of viewing or extracting the information. The output files are the same for both program versions.

A.1 *Antenna_FFT* Input File

A.1.1 Header

The input file for *Antenna_FFT* is shown in Appendix B. The first 7 lines are for informational purposes, and have no effect on the program. However, note that all variables are given in SI units, and that there must be 7 lines prior to the first variable defined.

A.1.2 Run Identifier (*run_id*)

The *run_id* is a 7 character variable used to name the 3 output files. The 3 output files are named

- 'sn'// *run_id*
- 'ed'// *run_id*
- 'xl'// *run_id.*

(The // represents FORTRAN90 string concatenation.) Output files are located in the local directory from which the program is run. A sample pattern for *run_id* is *run_id*='001_FFT'. Characters which Matlab® would interpret as operators (/, +, -, *, etc.) should be avoided in *run_id* if the Matlab® output option is selected.

A.1.3 FFT Power of 2 (*nnf*)

The FFT algorithm is designed to operate on arrays which have an integer power of 2 elements. *nnf* sets this power of 2, making

$$N\_sea = 2^{nnf} \tag{A.1}$$

where

N_sea is the number of sea frequency components and spatial locations.

The number of sea modeled in the spatial domain is generally much higher than the antenna length requires, however the speed advantage of the FFT method more than outweighs the penalty of carrying along the extra sea information.

A.1.4 Number of Antenna Elements (*num_of_elem*)

This is the number of physical antenna receiver elements in the array, assuming that

- the array is fully populated
- the elements have zero space between them.

A.1.5 Antenna Element Length (*element_length*)

This is the length of each antenna element.

A.1.6 Antenna Oversample Factor (M)

Each antenna element is broken down into an integer number, M, of sections. These sections correspond to the antenna spatial mesh size Δs. By enforcing the condition that $\Delta s = \Delta x$, the computer model constructs the spatial frequency meshing, Δb, such that

$$b_{\max} = \frac{1}{2\,\Delta s} \tag{A.2}$$

$$L\_sea = \Delta s\; N\_sea \tag{A.3}$$

$$\Delta b = \frac{1}{L\_sea} \tag{A.4}$$

By invoking the dispersion relation, we convert from the b domain to the ω domain, using

$$\omega = \sqrt{2\pi g b} \tag{A.5}$$

This process shows how the spatial meshing relates to the sea energy frequency domain meshing. As one can see, the fact that N_sea is constrained to be a power of 2 introduces some limitations on the mesh size Δs, since it is required that

$$element\_length = M\;\Delta s \tag{A.6}$$

A.1.7 Maximum Number of Samples (*max_ num_ of_ samples*)

This refers to the maximum number of "snapshots" taken for the Matlab® viewer, or the exposure data matrix. *max_ num_ of_ samples* is used to dynamically allocate array storage for variables which are sampled periodically in time.

A.1.8 Water Density (*rho_ water*)

Water density in which the antenna operates.

A.1.9 Antenna Density (*rho_ antenna*)

The average antenna density, which is assumed to be constant over the entire array. This is an approximation in that the prototype unit built by Lincoln Laboratory has slightly higher

density at the antenna element, and slightly lower density between elements.

A.1.10 Antenna Diameter (*diam_ antenna*)

This is the outer diameter of the hose-like structure encasing the antenna. Element performance (gain) is controlled by whether this outer diameter is submerged; the diameter of the inner conducting slot antenna affects the rotational invariance of the element, and the maximum theoretical gain of a fully exposed element.

A.1.11 Drogue Size (*drog_ area*)

The drogue frontal area (in m^2) determines the tension at the trailing end of the antenna, according to

$$T = \frac{1}{2}\rho_{water} U^2 \, drog\_area \, CD\_n \tag{A.7}$$

A value of 0.01 m^2 was used for all simulations.

A.1.12 Threshold Antenna Exposure (*reqd_ ant_ exposure*)

As mentioned earlier, the antenna gain remains steady until the element just becomes submerged. In order to capture this performance, and introduce margin for capillary waves not modeled, the parameter *reqd_ ant_ exposure* has been defined. The *reqd_ ant_ exposure* is the height above the water which must be maintained by the antenna to be considered exposed. The *reqd_ ant_ exposure* is given as a fraction of the antenna diameter. See Figure A-1 for a diagram representing an antenna diameter of 1.0 and a *reqd_ ant_ exposure* of 0.04. (0.04 is the value used on all simulation results presented.)

A.1.13 Tow Speed (U)

The tow speed of the antenna is assumed constant with respect to time. Tow speed must be greater than zero (in order to generate tension); direction of tow is specified with the next variable, *head_ seas*. For the case of stern seas only, sea frequency components above *omega_crit*,

$$omega\_crit = \frac{g}{U} \tag{A.8}$$

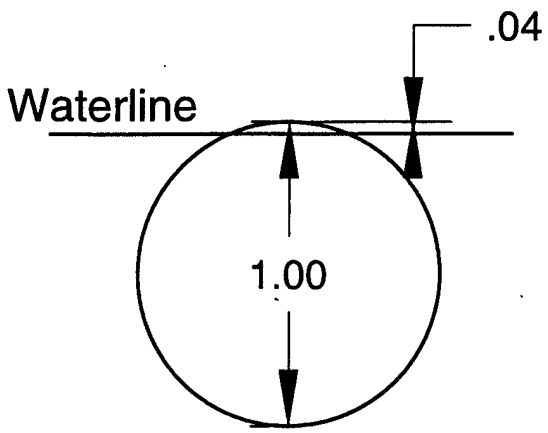

Figure A-1: Sample Threshold Antenna Exposure of 0.04

are zeroed out to prevent antenna folding. If *omega_crit* is less than 1.5 rad/sec, then a warning is issued that excessive frequency components are being zeroed out, and program execution stops.

A.1.14 Direction of Seas Option (*head_seas*)

The sea direction is limited to pure head seas or pure stern seas. *head_seas* is a logical variable: .TRUE. indicates towing into head seas ($U < 0$), and .FALSE. indicates towing with stern seas ($U > 0$). The sign of U is assigned internally by the program; U should always be positive when specified in the input file.

A.1.15 Normal Drag Coefficient (*CD_n*)

This represents the drag coefficient for a cylinder in cross flow. A constant value of 1.0 has been assumed.

A.1.16 Tangential Drag Coefficient (*CD_t*)

This is the skin friction associated with flow along the long axis of the antenna. A relatively smooth outer surface has been assumed in choosing this value, which has been assumed constant.

(0.0035 used in all simulations.)

A.1.17 Added Mass Coefficient (C_m)

The added mass coefficient for a cylinder in cross flow has been set to 2.0.

A.1.18 Simulation Time (*duration*)

The total length of time simulated by the program. While many factors affect the actual time necessary to perform the simulation (antenna length, number of mesh points, CPU speed, etc.), the ratio of actual time to simulation time is roughly 5:1. (For the SWS version, the ratio is roughly 50:1.)

A.1.19 Time Margin (*margin*)

The time step size used by the program, t_incr, is given by

$$t\_incr = margin\frac{\Delta s}{c} \tag{A.9}$$

where c is the string wave propagation velocity

$$c = \sqrt{\frac{T}{\rho_{ant}\,\pi\frac{D^2}{4}}} \tag{A.10}$$

and

T is the string tension

ρ_{ant} is the antenna density

D is the antenna diameter.

The tension used initially to estimate the time step is the calm water (local fluid particle velocity, $u = 0$) tension at the tow point. When $dynamic\_tension$ = .TRUE., then the actual tension varies with x and t as the actual wetted surface area changes, and as the local fluid particle velocity, u, evolves along the length of the antenna. A sample plot of maximum tow point tension vs. significant wave height using the parameters of Table A.1 is provided in Figure A-2. As can be seen in the figure, the maximum tow point tension in a 3.0 m significant wave

Parameter	Description
Method	SWS
H_s	various
Devel	1.0
$\omega_{\min}$	0.4 rad/sec
$\omega_{\max}$	24.0 rad/sec
N_{freq}	700
L	25 m
N_{elem}	50
L_{elem}	0.5 m
M	8
Δs	0.0625 m
Diameter	3.0 inch
ρ_{ant}	408 kg/m^3
EI	0 Pa m^4
Duration	180 sec
U	5 kts
N_{thresh}	40

Table A.1: Tension Input Parameters

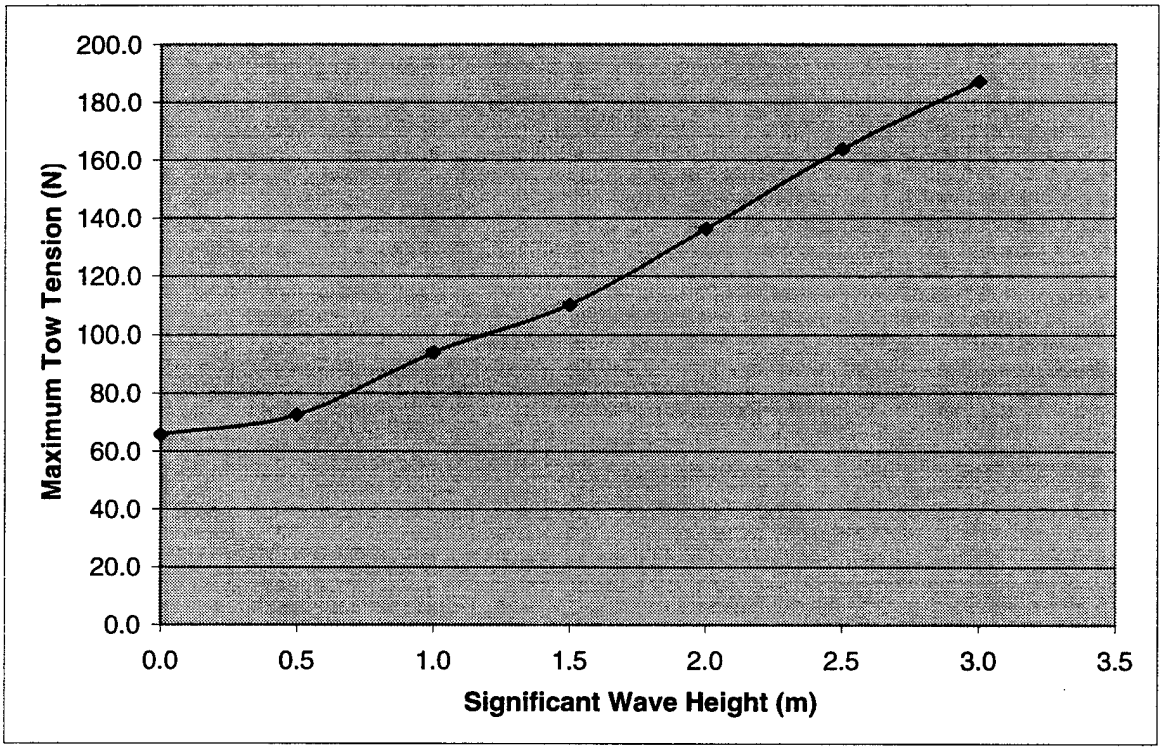

Figure A-2: Variation of Maximum Tow Point Tension vs. Significant Wave Height

height sea is about triple that of the calm water value. This would lead to a required value for *margin* of $\frac{1}{\sqrt{3}}$, or about 0.58. In practice, a value of 0.25 to 0.33 was used; however, no detailed effort was made to determine the maximum value allowed for *margin*.

For the case of *dynamic_tension* = .FALSE., the calm water tow tension is also the maximum tow tension. (Tension is determined entirely by a relative fluid velocity of U, and the wetted area corresponding to the calm water submergence depth.) Thus a value much closer to 1.0 is possible for *margin*.

When the antenna is modeled as having lateral stiffness (i.e. *flex_stiff_coef* > 0.0), the variable *margin* is used to empirically determine a satisfactory time increment. Time step size is quite sensitive to antenna stiffness, and *margin* must reduced an order of magnitude for typical designs considered (e.g. *flex_stiff_coef* =100 Pa m^4).

A.1.20 Snapshot Output Interval (*pic_time*)

This variable allows the user to control the time interval between snapshots, which are recorded to file 'sn'//*run_id*. These snapshots record both the sea and antenna elevation data along the entire length of the antenna, at a resolution of Δs. A Matlab® viewer script file is included in Appendix D, which allows the user to step through the snapshots frame by frame. *pic_time* has been set to 1.0 second for all run results presented.

A.1.21 Time of First Snapshot (*t_first_pic*)

The time to begin recording snapshots is user defined. This is useful to ignore transient behavior at the start of the simulation, or to save only a representative sample at the end of a lengthy simulation.

A.1.22 Statistics Output Interval (*stat_time*)

This variable allows the user to control the time interval between exposure data matrix records, which are recorded to file 'ed'//*run_id*. While *stat_time* is independent of *pic_time*, a value of 1.0 second was also used for this variable for all simulations. Selection of a *stat_time* excessively small results in subsequent records containing essentially the same information, and contributes little to the statistics of the sample.

A.1.23 Threshold Number of Elements (*num_of_elem_thresh*)

This variable allows the user to specify the lowest number of exposed antenna elements necessary to achieve the desired design antenna array gain. At each *stat_time*, the number of exposed elements is compared to *num_of_elem_thresh*; the result (a "1" when the threshold is met, "0" otherwise) is written at the end of the summary output file, 'xl'//*run_id*, along with any other variables tracked over the course of the simulation. Currently, the variables tracked over time are

- tow point tension (*tow_tension*( ))
- number of elements exposed (*is_exposed*(,))
- threshold met (*thresh_met*: "0" or "1", as above)
- counterdetection length (*length_totally_exposed*( )).

A.1.24 Tension Model Option(*dynamic_tension*)

(See discussion under Section A.1.19.)

A.1.25 Snapshot Output Option(*matlab_output*)

The snapshot output file ('sn'//*run_id*) is optional, since it does not contain any unique statistical information, and requires a relatively large amount of disk space. (Average file size is about 1.4 MB for a 180 second simulation.) The primary benefit of examining the snapshot output file is to learn the physical behavior of the antenna in a seaway. In addition, the output is useful to detect when the time step size is too small, which is characterized by rapid unphysical antenna oscillations. *matlab_output*=.TRUE. means that snapshot output is enabled, .FALSE. means snapshot output is disabled.

A.1.26 Significant Wave Height (*sig_wave_ht*)

This variable sets the sea's significant wave height, a parameter used to describe the sea severity in both the Bretschneider and Ochi spectral models. Appendix E correlates sea state to significant wave height for a fully developed sea.

A.1.27 Development (*development*)

As discussed in Section 2.1.2, this variable allows the user to shift the sea spectral energy modal frequency up (for developing seas) or down (for decaying seas). This parameter applies only to the Bretschneider spectral model.

A.1.28 Spectral Model (*spectral_model*)

Two spectral model subroutines are available: the two parameter Bretschneider spectrum, and the Ochi "most probable" six parameter spectrum. ("1" means Bretschneider, "2" means Ochi.) The Bretschneider spectral model was used for all simulations presented.

A.1.29 Antenna Lateral Stiffness (*flex_stiff_coef*)

This variable represents the resistance of the antenna to bending, and is given by

$$flex\_stiff\_coef = EI \tag{A.11}$$

where

E is the modulus of elasticity

I is the area moment of inertia.

A.2 Input File Features Unique to *Antenna_SWS*

The differences in the Antenna_SWS input file pertain to the discretization of the sea circular frequency components.

A.2.1 Number of Sea Frequency Components (*num_of_freqs*)

This variable is the number of discrete sea frequency components in the spectrum. *num_of_freqs* = 700 was used for the simulations, however as few as about 100 components provide adequate sea representation. The frequency components are evenly spaced in the ω domain.

A.2.2 Frequency Coverage (*omega_min, omega_max*)

The frequency components ω_i are evenly spaced from *omega_min* to *omega_max*. For the simulations presented *omega_min* = 0.4 rad/sec and *omega_max* = 24.0 rad/sec.

A.2.3 Spectral Model (*spectral_model*)

One extra option is added: for *spectral_model* = 3, the sea surface is described by a pure harmonic wave of amplitude *sig_wave_ht* and circular frequency *omega_max*.

A.3 Output Files

A.3.1 End-State Summary File ('xl'//*run_id*)

This file provides

- a printout of forces, velocities, and positions at the end of the run
- a record of the input parameters used for the simulation
- averaged statistics results, and
- a time history of variables tracked by the program.

This file is suitable for viewing with a spreadsheet application, such as Microsoft Excel®.

A.3.2 Exposure Data Matrix File ('ed'//*run_id*)

This file, whose data structure is given in Table 4.1, contains the raw exposure data information for each antenna element at each time sampled. This allows one to analyze statistics across time or space. This file is easily analyzed by a spreadsheet application.

A.3.3 Snapshot File ('sn'//*run_id*)

The snapshot file can be viewed with a user written code, or by *Snaps.m*, a simple Matlab® routine provided in Appendix D. It provides views of the antenna as it floats on the surface at two scales: one view is large enough to see the most extreme waves, one zooms in on the sea

surface by using the local water elevation as the zero for the z axis. The latter view also shows the antenna central axis, the antenna upper limit, and the antenna lower limit.

Appendix B

Input File for *Antenna_FFT*

```
Input File for Antenna_FFT Simulation Program

SI units throughout; useful conversions follow
1 inch = 0.0254 m
1 foot = 0.3048 m
1 knot = 0.5144 m/s

000_FFT     run_id              7 characters long
13          nnf                 # of components. N_sea=2**nnf
25          num_of_elem         # of actual slotted antenna elements
0.5         element_length      physical slotted antenna length (m).
8           M                   # of mesh points/element_length.
300         max_num_of_samples  to dimension time arrays
1025.9      rho_water           seawater at 15 deg C (kg/m^3)
408.0       rho_antenna         density of antenna (kg/m^3)
0.0762      diam_antenna        antenna outer diameter (m)
0.01        drog_area           drogue area normal to flow (m^2)
0.04        reqd_ant_exposure   threshold vertical exposure for reception. (x/diameter)
2.5722      U                   tow speed (use POSITIVE #) (m/s)
.TRUE.      head_seas           TRUE: antenna is towed into head seas
1.0         CD_n                normal flow drag coefficient
0.0035      CD_t                fluid tangential drag coefficient (p. 50 Berteaux)
2.0         C_m                 added mass coefficient
4.0         duration            total simulated run time (sec)
0.27        margin              saftey factor applied to time step size
1.0         pic_time            snapshot interval for Matlab viewer (sec)
0.0         t_first_pic         time of first snapshot (sec)
1.0         stat_time           statistics interval (sec)
```

```
20          num_of_elem_thresh  # of exposed elements reqd for specified gain
.TRUE.      dynamic_tension     FALSE: steady-state calm water model to find tension
.TRUE.      matlab_output       TRUE: Matlab viewer output is ON
2.5         sig_wave_ht         significant wave height (m)
1.0         development         modal frequency shift factor
1           spectral_model      1=Bretschneider; 2=Ochi
0.0         flex_stiff_coef     E*I (Pa m^4)
```

Appendix C

Input File for *Antenna_SWS*

```
Input File for Antenna_SWS Simulation Program

SI units throughout; useful conversions follow
1 inch = 0.0254 m
1 foot = 0.3048 m
1 knot = 0.5144 m/s

000_SWS     run_id              7 characters long
25          num_of_elem         # of actual slotted antenna elements
0.5         element_length      physical slotted antenna length (m).
8           M                   # of mesh points/element_length.
100         num_of_freqs        # of discrete freq components
300         max_num_of_samples  to dimension time arrays
1025.9      rho_water           seawater at 15 deg C (kg/m^3)
408.0       rho_antenna         density of antenna (kg/m^3)
0.0762      diam_antenna        antenna outer diameter (m)
0.01        drog_area           drogue area normal to flow (m^2)
0.04        reqd_ant_exposure   threshold vertical exposure for reception. (x/diameter)
2.5722      U                   tow speed (use POSITIVE #) (m/s)
.TRUE.      head_seas           TRUE: antenna is towed into head seas
1.0         CD_n                normal flow drag coefficient
0.0035      CD_t                fluid tangential drag coefficient (p. 50 Berteaux)
2.0         C_m                 added mass coefficient
4.0         duration            total simulated run time (sec)
0.27        margin              saftey factor applied to time step size
1.0         pic_time            snapshot interval for Matlab viewer (sec)
0.0         t_first_pic         time of first snapshot (sec)
1.0         stat_time           statistics interval (sec)
```

```
20          num_of_elem_thresh  # of exposed elements reqd for specified gain
.TRUE.      dynamic_tension     FALSE: steady-state calm water model to find tension
.TRUE.      matlab_output       TRUE: Matlab viewer output is ON
0.40        omega_min           lower cutoff freq of sea spectrum (rad/sec)
15.0        omega_max           upper cutoff freq of sea spectrum (rad/sec)
2.5         sig_wave_ht         significant wave height (m)
1.0         development         modal frequency shift factor
1           spectral_model      1=Bretschneider; 2=Ochi; 3=pure sine wave
0.0         flex_stiff_coef     E*I (Pa m^4)
```

Appendix D

Source Code Listing for *Snaps.m*

```
! snaps   displays antenna and sea surface as a series of snapshots

! displays series of antenna snapshots

! N=number of antenna elements
! M=number of snapshots taken

! number of rows in file = M+1
! number of cols in file = 2*N+1

! File format (ASCII)
! col 1:
!   zero (a dummy), time 1, ... , time M
! col 2:
!   x(1), z(1) at time 1, ... , z(1) at time M
! col N+1:
!   x(N), z(N) at time 1, ... , z(N) at time M
! col N+2:
!   x(1), h(1) at time 1, ... , h(N) at time M
! col 2*N+1:
!   x(N), h(N) at time 1, ... , h(N) at time M

clear
load sn000_SWS -ascii

[M,N]=size(sn000_SWS);
N=(N-1)/2;
M=M-1;
```

```
t=sn000_SWS(2:M+1,1);
x=sn000_SWS(1,2:N+1);
z=sn000_SWS(2:M+1,2:N+1);
h=sn000_SWS(2:M+1,N+2:2*N+1);
diam=sn000_SWS(1,1);
y=z-h;
for j=1:N
   zz(j)=0.0;
   thresh1(j)=0.04*diam;
   thresh2(j)=-0.04*diam;
end

! find max/min z for consistent plot scales
z_min=min(h);                  ! z_min is a row vector
z_min=min(z_min);              ! z_min is now a scalar
z_max=max(h);
z_max=max(z_max);
figure(1);
for j=1:M
   if j>1
      pause;
   end
   subplot(2,1,1);
   plot(x,z(j,:),x,h(j,:), x,zz);
   title(['Time', blanks(3),num2str(t(j))]);
   ylabel('z, h  (m)');
   axis([0.0 x(N) z_min z_max]);
   subplot(2,1,2);
   plot(x,y(j,:),'k:',x,thresh1,'b-',x,thresh2,'b-',x,zz,'g-');
   axis([0.0 x(N) -.05 .05]);
   xlabel('x (meters)');
   ylabel('y = z - h  (m)');

end
```

Appendix E

Sea State Data for Fully Arisen Seas

Significant Wave Height (m)	Modal Frequency (rad/sec)	Wind Speed (knots)	Sea State
0.1	3.96	4.2	
0.2	2.80	5.9	
0.3	2.29	7.3	1
0.4	1.98	8.4	
0.5	1.77	9.4	
0.6	1.62	10.3	
0.7	1.50	11.1	
0.8	1.40	11.9	2
0.9	1.32	12.6	
1.0	1.25	13.3	
1.1	1.20	13.9	
1.2	1.14	14.6	
1.3	1.10	15.2	3
1.4	1.06	15.7	
1.5	1.02	16.3	
1.6	0.99	16.8	
1.7	0.96	17.3	
1.8	0.93	17.8	
1.9	0.91	18.3	
2.0	0.89	18.8	4
2.2	0.85	19.7	
2.4	0.81	20.6	
2.6	0.78	21.4	
2.8	0.75	22.2	
3.0	0.72	23.0	5
3.2	0.70	23.8	
3.4	0.68	24.5	
3.6	0.66	25.2	6
3.8	0.64	25.9	
4.0	0.63	26.6	
4.5	0.59	28.2	
5.0	0.56	29.7	
5.5	0.53	31.2	
6.0	0.51	32.6	
6.5	0.49	33.9	7
7.0	0.47	35.2	
7.5	0.46	36.4	
8.0	0.44	37.6	
8.5	0.43	38.8	
9.0	0.42	39.9	

Table E.1: Sea State Data for a Fully Arisen Sea

Bibliography

[1] "Recommended FY 00 Advanced Technology Demonstrations," *Inside the Navy*, August 3, 1998.

[2] Ochi, M. K. (1998). *Ocean Waves.* Cambridge University Press, London.

[3] Pierson, W. J. and Moskowitz, L. (1964). "A proposed spectral form for fully developed wind seas based on the similarity theory of S. A. Kitaigorodskii." Journal of Geophysical Res., Vol. 69, No. 24, pp. 5181-90.

[4] Bretschneider, C. L. (1959). "Wave variability and wave spectra for wind-generated gravity waves." Tech. Memo. No. 118 Beach Erosion Board, US Army Corps of Engineers, Washington, DC.

[5] Ochi, M. K. and Hubble, E. N. (1976). "On six parameter wave spectra." Proc. 15th Conf. Coastal Engineering., Vol. 1, pp. 301-28.

[6] Hasselmann, K. et al. (1973). "Measurements of wind-wave growth and swell decay during the Joint North Sea Wave Project (JONSWAP)." Deutschland Hydrographic Institute, Hamburg.

[7] Bouws, E. et al. (1985). "Similarity of the wind wave spectrum in finite depth water: 1. Spectral form." Journal Geophysical Res., Vol. 90, No. C1, pp. 975-86.

[8] Wilson, B. W. (1960). "Characteristics of anchor cables in uniform ocean currents." Texas A&M Tech. Report 204-1.

[9] Newman J. N. (1992). *Marine Hydrodynamics,* MIT Press, Cambridge, MA

[10] Ulrich, G. A., "Source Code for a Computer Model for a Towed Submarine Communication Antenna," MIT Department of Ocean Engineering Report 99-1, May 1999.

[11] Celia, M. A. and Gray, W. G. (1992). *Numerical Methods for Differential Equations.* Prentice Hall, Englewood Cliffs, New Jersey.

[12] Lincoln Laboratory, "UHF Antenna Element," Program Review, December 17, 1998.